iScience

CellPress
OPEN ACCESS

Article

Primate Amygdalo-Nigral Pathway for Boosting Oculomotor Action in Motivating Situations

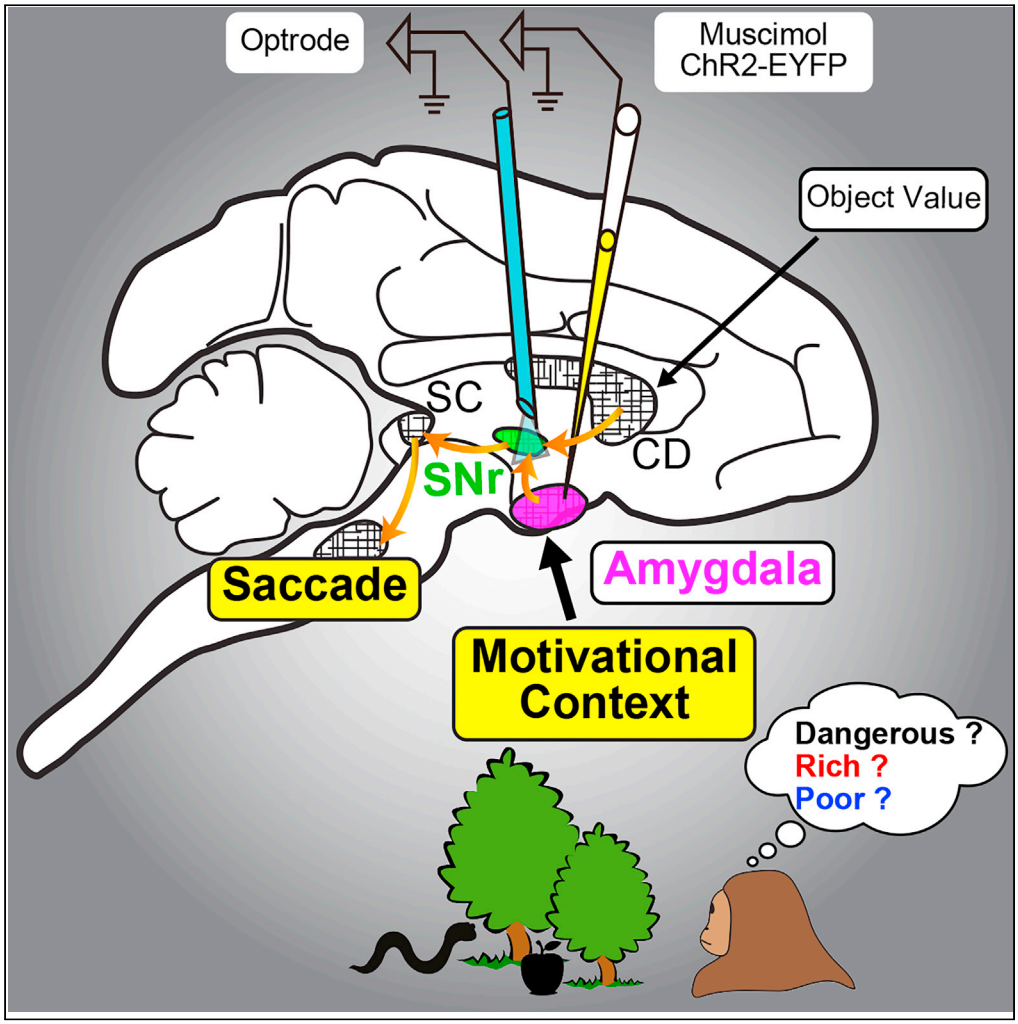

Kazutaka Maeda,
Ken-ichi Inoue,
Jun Kunimatsu,
Masahiko Takada,
Okihide Hikosaka

kaz.maeda.86@gmail.com
(K.M.)
oh@lsr.nei.nih.gov (O.H.)

HIGHLIGHTS

Amygdala facilitates saccades and gaze to the contralateral side

This is mediated by direct inhibitory connection to substantia nigra pars reticulata

Motivational context is transmitted through this pathway to control saccade and gaze

Amygdala thus controls goal-directed behavior using the basal ganglia circuit

Maeda et al., iScience 23, 101194
June 26, 2020
https://doi.org/10.1016/j.isci.2020.101194

iScience

CellPress
OPEN ACCESS

Article

Primate Amygdalo-Nigral Pathway for Boosting Oculomotor Action in Motivating Situations

Kazutaka Maeda,[1,6,*] Ken-ichi Inoue,[2,3] Jun Kunimatsu,[1,4,5] Masahiko Takada,[2] and Okihide Hikosaka[1,*]

SUMMARY

A primary function of the primate amygdala is to modulate behavior based on emotional cues. To study the underlying neural mechanism, we first inactivated the amygdala locally and temporarily by injecting a GABA agonist. Then, saccadic eye movements and gaze were suppressed only on the contralateral side. Next, we performed optogenetic activation after injecting a viral vector into the amygdala. Optical stimulation in the amygdala excited amygdala neurons, whereas optical stimulation of axon terminals in the substantia nigra pars reticulata inhibited nigra neurons. Optical stimulation in either structure facilitated saccades to the contralateral side. These data suggest that the amygdala controls saccades and gaze through the basal ganglia output to the superior colliculus. Importantly, this amygdala-derived circuit mediates emotional context information, whereas the internal basal ganglia circuit mediates object value information. This finding demonstrates a basic mechanism whereby basal ganglia output can be modulated by other areas conveying distinct information.

INTRODUCTION

Eye movements are important for scanning the visual environment and making decisions. Abnormal eye movement patterns are a common symptom in many psychiatric disorders, including attention-deficit/hyperactivity disorder, bipolar disorder, and autism (Constantino et al., 2017; Munoz et al., 2003; Yep et al., 2018). Amygdala abnormalities are thought to be a key factor in these disorders (Avino et al., 2018; Davis and Whalen, 2001); however, it remains unknown whether the amygdala dysfunction and oculomotor symptoms are related to each other. Some studies have shown that amygdala lesions alter gaze patterns, especially for face images (Dal Monte et al., 2015; Taubert et al., 2018). Moreover, amygdala neurons are spatially selective and encode information about both the location and the motivational significance of visual cues (Peck and Salzman, 2014). As spatial attention is tightly coupled to motor function, especially in the case of stimulus-driven orienting behaviors (Corbetta and Shulman, 2002), it is plausible that amygdala neurons convey signals appropriate for control of eye movements. However, causal evidence linking the amygdala to abnormal eye movement patterns is lacking in both human and animal studies.

We have recently demonstrated that amygdala neurons, mostly in the central nucleus (CeA), encode emotional contexts (dangerous versus safe, rich versus poor) (Maeda et al., 2018). Importantly, we found that the activity of amygdala neurons was negatively correlated with the reaction time of saccadic eye movements to reward-associated objects. Anatomical studies have reported that the amygdala sends output to the basal ganglia, including the caudate tail (CDt), the globus pallidus externus (GPe), and the substantia nigra pars reticulata (SNr) (Fudge and Haber, 2000; Griggs et al., 2017; Price and Amaral, 1981; Shinonaga et al., 1992; Vankova et al., 1992). These structures are known to comprise a circuit that encodes the stable values of objects learned through long-term experience and also controls saccades through the SNr-superior colliculus (SC) pathway (Amita et al., 2019; Griggs et al., 2017). This suggests that amygdala neurons modulate saccadic eye movements by sending contextual information to the basal ganglia circuit.

Here we assessed the impact of motivating contexts on amygdala neuron activity through electrophysiological recordings and explored its relation to saccadic eye movements in a foraging task. Saccades to the contralateral side were strongly suppressed by muscimol-induced inactivation and enhanced by optogenetic activation of the amygdala. The results indicate that the amygdala controls the saccade and gaze

[1]Laboratory of Sensorimotor Research, National Eye Institute, National Institutes of Health, Bethesda, MD 20892, USA

[2]Systems Neuroscience Section, Primate Research Institute, Kyoto University, Inuyama, Aichi 484-8506, Japan

[3]PRESTO, Japan Science and Technology Agency, Kawaguchi, Saitama 332-0012, Japan

[4]Division of Biomedical Science, Faculty of Medicine, University of Tsukuba, Tsukuba, Ibaraki 305-8577, Japan

[5]Transborder Medical Research Center, University of Tsukuba, Tsukuba, Ibaraki 305-8577, Japan

[6]Lead Contact

*Correspondence: kaz.maeda.86@gmail.com (K.M.), oh@lsr.nei.nih.gov (O.H.)

https://doi.org/10.1016/j.isci.2020.101194

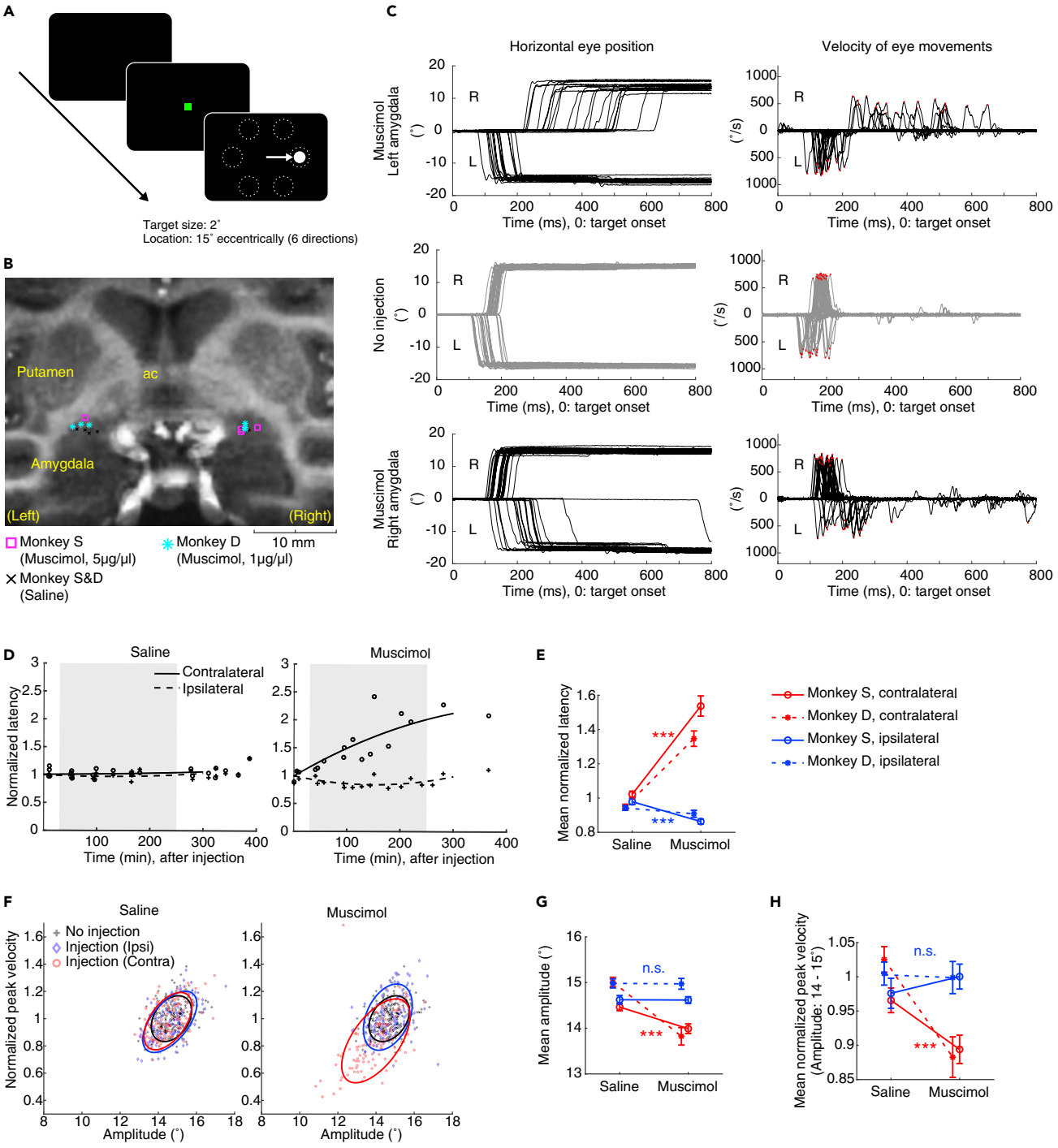

Figure 1. Changes in Saccade Features by Amygdala Inactivation

(A) Visually guided saccade task.

(B) Estimated injection sites in the central nucleus of amygdala. ac, anterior commissure.

(C) Horizontal eye position (left) and velocity (right) after target onset (red dots: the peak velocity in each saccade).

(D) Changes in saccade latency after injection of saline (left) and muscimol (right). Shaded gray area shows the effective period we used for further analysis (each data point: averaged saccade latency in each session). Solid and dashed lines indicate second-degree least-squares fit to the data points for contralateral and ipsilateral, respectively.

(E) Mean latency in each condition. The data were obtained from individual trials during the effective period.

Figure 1. *Continued*

(F) Relationship between saccade amplitude (abscissa) and peak velocity (ordinate). Solid lines show 70% confidence ellipse in each condition (black: no injection, red: CeA inactivation—contralateral saccades, blue: CeA inactivation—ipsilateral saccades).

(G) Mean saccade amplitude.

(H) Mean saccade peak velocity. Error bars show SEM. Asterisk (***) indicates statistically significant contrasts at $p < 0.001$ (two-sample t test). All data in C, D, and F are for monkey S (Figure S1 show original data for both monkeys S and D).

position in a spatially selective manner. Furthermore, we provide evidence for the amygdala-SNr (amygdalo-nigral) pathway to control spatial attention and action in motivating contexts.

RESULTS

Suppression of Saccades by Amygdala Inactivation

We first examined the behavioral function of the amygdala by temporarily inactivating amygdala neurons through local injection of muscimol, a $GABA_A$ receptor agonist (Hikosaka and Wurtz, 1985a, b). Before and after the muscimol injection (8.8 or 44 nmol [1μg or 5 μg] in a 1μL volume), monkeys performed a visually guided saccade task (Figure 1A). Before each injection, we identified the amygdala physiologically by recording neuronal activity using an injectrode (polyimide tube attached to a recording electrode for drug delivery, see Methods). We carried out 8 unilateral injections in monkey S (44 nmol [5μg] muscimol: 4 times, saline: 4 times) and 12 unilateral injections in monkey D (8.8 nmol [1 μg] muscimol: 6 times, saline: 6 times) (Table S1). Figure 1B shows the injection sites that appeared to be located in an amygdala sector corresponding to CeA in a magnetic resonance (MR) image.

In the visually guided saccade task, unilateral injections of muscimol into the amygdala suppressed contralateral saccades. Examples from a typical session are shown in Figure 1C: left amygdala inactivation (Figure 1C, top) increased the latencies of saccades to the right (contralateral) target compared with control data (Figure 1C, middle). Moreover, the saccade peak velocity decreased during such delayed saccades (Figure 1C, top right). In contrast, the saccade velocity to the left (ipsilateral) target was unchanged, although latencies were slightly shortened. Right amygdala inactivation (Figure 1C, bottom) produced similar effects: longer latencies and lower peak velocities for saccades to the left (contralateral) target and slightly shorter latencies for saccades to the right (ipsilateral) target.

We repeated the same experiment with varying delays after muscimol injections. The effect of muscimol on saccade latency started immediately and increased over time within a daily session (Figures 1D and S1A for original data). We analyzed the data in an effective period (30–250 min after the injection) and compared with the effect in the same window in control experiments (saline injection). The latency increased significantly on the contralateral side during amygdala inactivation, and the results were similar in both monkeys (Figure 1E, two-sample t test, $T(397) = -11.385$, $p = 3.518 \times 10^{-26}$, individual statistics values written below are also shown in Table S2). On the ipsilateral side, the latency tended to decrease during amygdala inactivation.

In addition to the latency changes described above, the amplitude of contralateral saccades sometimes became smaller (Figures 1F and 1G, two-sample t test, $T(397) = 6.7242$, $p = 6.1672 \times 10^{-11}$), i.e., hypometric following the muscimol injection (Figure 1C, top and bottom) compared with control data (Figure 1C, middle). We considered the possibility that the lower peak velocity of contralateral saccades might simply be correlated with smaller saccade amplitudes according to the main sequence (Pearson's correlation, $r > 0$, $p < 0.05$) (Figure 1F), a well-known property of saccades (Baloh et al., 1975; Robinson, 1964). To test this possibility, we compared the peak velocity within a short range of saccade amplitude (14–15°) and found that the peak velocity still significantly decreased following inactivation of the amygdala in both monkeys (Figure 1H, two-sample t test, $T(112.8057) = 4.6518$, $p = 9.0142 \times 10^{-6}$). These data indicate that inactivation of the amygdala alters three properties of contralateral saccades: (1) increase in latency; (2) decrease in amplitude; and (3) decrease in peak velocity.

Our data showed that inactivation of the amygdala suppressed oculomotor behaviors. However, this effect might be caused by the inactivation of surrounding areas, especially the caudal-ventral part of the putamen, which we call "putamen tail (PUTt)" where neurons encode stable object values (Kunimatsu et al., 2019). We thus injected muscimol in PUTt unilaterally (monkey S: n = 3, monkey D: n = 4) (Figure S2A). Although the saccade latency increased after muscimol injections in PUTt (nested data: $p = 1.5389 \times 10^{-10}$, monkey

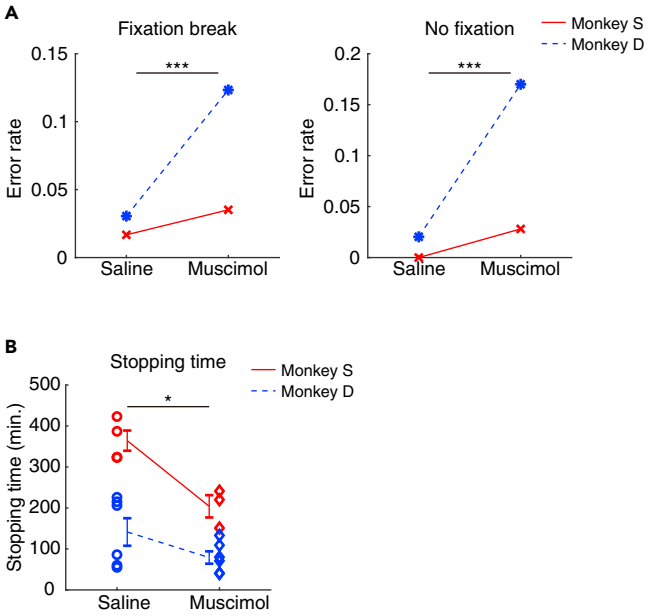

Figure 2. Motivational Deficits during Goal-Directed Behavior Following Amygdala Inactivation

(A) Increase in fixation error rate before saccade target appeared: fixation breaks (left) and no fixation trials (right).

(B) Earlier termination of the visually guided saccade task following amygdala inactivation. The stopping time was defined as the point at which the monkey failed to make the initial fixation on five consecutive trials over the course of an injection session. When no such sequence of failures occurred, the end of planned experimental session was taken as the stopping time (monkey S: 364.25 ± 49.30 min, monkey D: 131.29 ± 79.74 min in the control session). Each marker indicates the stopping time in each injection experiment (red: monkey S, blue: monkey D). Error bars show SEM; asterisks (*) and (***) indicate statistically significant contrasts at $p < 0.05$ and $p < 0.001$. related to Figure 1.

S: $p = 3.8975 \times 10^{-7}$, monkey D: $p = 2.3778 \times 10^{-6}$), the effects were weaker and shorter than after muscimol injections in amygdala (nested data: $p = 9.8533 \times 10^{-5}$, monkey S: $p = 0.15483$, monkey D: $p = 1.558 \times 10^{-5}$) (Figures S2B and S2C). We also injected muscimol in GPe (i.e., dorsal to amygdala), which again caused only weak effects on saccade latency (Figure S2B, right). We decided not to repeat this experiment because it caused long-lasting contralateral hemiplegia (around 2 weeks) with no further change in saccades, suggesting that this part of GPe controls body movements rather than eye movements. These data suggest that the full strength of the effects of muscimol on saccades must indeed be due to the amygdala inactivation.

The saccade deficits might be caused by the dysfunction of visual perception rather than the dysfunction of oculomotor control. To test this possibility, we used the value-based visually guided saccade task (Figure S3A). Two dots in different colors were used as the good and bad objects, which were associated with large and small rewards. Normally (with no or saline injection), the monkeys made saccades quickly (short latency) to the good object and slowly (long latency) to the bad object (Figure S3B, left), as shown previously (Kim and Hikosaka, 2013; Yamamoto et al., 2013). After muscimol injection into the amygdala, the saccade latency increased for both objects on the contralateral side. However, it remained shorter for the good object than for the bad object on both the ipsilateral and the contralateral sides (Figure S3B, right). The data suggest that the visual perception of the target in the visually guided saccade task (Figure 1A) was kept intact even after the amygdala inactivation.

Inactivation of the amygdala also disrupted the monkeys' goal-directed visual behavior in ways not captured by the saccade metrics described above. On each trial of the visually guided saccade task (Figure 1A), the monkey needed to wait for the reward-associated object by maintaining gaze fixation on a central dot (770 ms), otherwise the trial ended with no opportunity for reward. Such adequate fixation was disrupted by amygdala inactivation in both monkeys (Figure 2A), in that they often broke fixation on the central dot before the object appeared (fixation break, nested data: $p = 6.8931 \times 10^{-5}$, monkey S: $p = 0.13588$, monkey D: $p = 2.2485 \times 10^{-5}$) or failed to look at the fixation point altogether (no fixation, nested data: $p = 4.9368 \times 10^{-10}$, monkey S: $p = 0.0034666$, monkey D: $p = 5.5859 \times 10^{-10}$). These effects, together

with the preceding results (Figure 1), suggest that the amygdala contributes to the goal-directed behavior both by suppressing inappropriate saccades in the absence of valid targets and by facilitating appropriate saccades after targets appear.

Under normal conditions, the monkeys were sufficiently motivated to perform behavioral tasks continually for long durations. After muscimol injection into the amygdala, however, the monkeys were more prone to quit performing the tasks we tested, including the visually guided saccade task (Figure 2B, mean stopping time (saline versus muscimol): 230.5 min versus 120.7 min after the injection, nested data: $p = 0.04047$, monkey S: $p = 0.0088632$, monkey D: $p = 0.13501$). This result suggests that the amygdala may play a role in motivational activation of goal-directed behavior. We consider this possibility in the next section.

Gaze Shift during Amygdala Inactivation

Under natural viewing conditions, eye movements are used to look at things sequentially according to the animal's attentional and motivational states as well as object saliency (Corbetta et al., 1998; Hoffman and Subramaniam, 1995; Taubert et al., 2018). To test whether the amygdala contributes to such behavior, we let monkeys watch a video clip freely without any reward (free-viewing task, duration: 5 min, see Methods and Figure 3A). Each image in Figure 3B shows eye positions of one monkey (S) during the 5-min free-viewing task. The duration of gaze (i.e., fixation between saccades) is indicated by color map. Without inactivation (Figure 3B center), monkey's gaze was distributed in various positions but was more common around the center. In contrast, during left or right amygdala inactivation (Figure 3B, left or right), gaze was mostly on the left (ipsilateral) or right (ipsilateral) side, respectively. The bias toward gaze shifts to the ipsilateral side was significant in both monkeys (Figures 3B and S4A, also 3C). These results may be characterized as "contralateral hemineglect" (Behrmann et al., 1997; Miyashita et al., 1995).

Amygdala inactivation also had general effects on saccadic eye movements (Figures 3D–3F). First, the frequency of saccades decreased, as reflected by an increased inter-saccade interval (ISI) (Figure 3D). These results indicate that saccadic eye movements were generally suppressed, whereas gaze tended to stay on the ipsilateral side. This effect may be related to attention and motivation (see Discussion). Second, saccades became slower. Because the saccade amplitude varied during free viewing, the relationship between the saccade velocity and the amplitude was well estimated in each of four conditions (Figure 3E). The peak velocity was positively correlated with the amplitude in all conditions (Pearson's correlation, $r > 0$, $p < 0.001$). However, the slope of the regression line decreased significantly only in contralateral saccades during amygdala inactivation (Figure 3F, ANCOVA and post hoc: least significant difference). These results indicate that the saccade peak velocity decreased across different amplitudes only in saccades directed to the side contralateral to the amygdala inactivation, which also confirmed the conclusion based on explicitly prompted saccades to targets in the visually guided saccade task (Figure 1).

Optogenetic Activation of Amygdala

To further investigate the role of the amygdala in eye movement control and shed light on the neural pathways involved, we injected an adeno-associated virus type 2 vector (AAV2-CMV-ChR2-EYFP) into the amygdala of one hemisphere in both monkeys (monkey S: left, monkey D: right, Table S3). Figure 4A shows the expression of ChR2-EYFP in monkey D. Many ChR2-positive neurons were found in the amygdala, corresponding to its central nucleus (CeA), which was similar to the muscimol injection sites (Figure 1B). In order to gauge the efficiency of viral labeling, we counted the fraction of NeuN-positive cells that expressed ChR2-EYFP (example cells are shown in Figure S5A). Near centers of injection sites (0.5 mm × 0.5 mm), 55.7% (59/106) of the NeuN-positive cells expressed ChR2-EYFP. Thus, the viral vector enabled the expression of ChR2-EYFP in amygdala neurons of the monkey.

One month after the injections, we tested the effect of stimulation at the viral vector injection sites using optrodes to deliver 473-nm blue laser light while simultaneously recording single neuron activity in the amygdala, mostly in CeA (monkey S, $n = 7$; monkey D, $n = 11$, Figure S5B). Many of the neurons (13 of 18, monkey S, $n = 7$; monkey D, $n = 6$) were modulated by the stimulation, mostly with excitatory responses (11 of 13, monkey S: 5, monkey D: 6), indicating that the excitatory opsin was successfully expressed in this area. A representative neuron is shown in Figure 4B (left), which was excited tonically during the stimulation

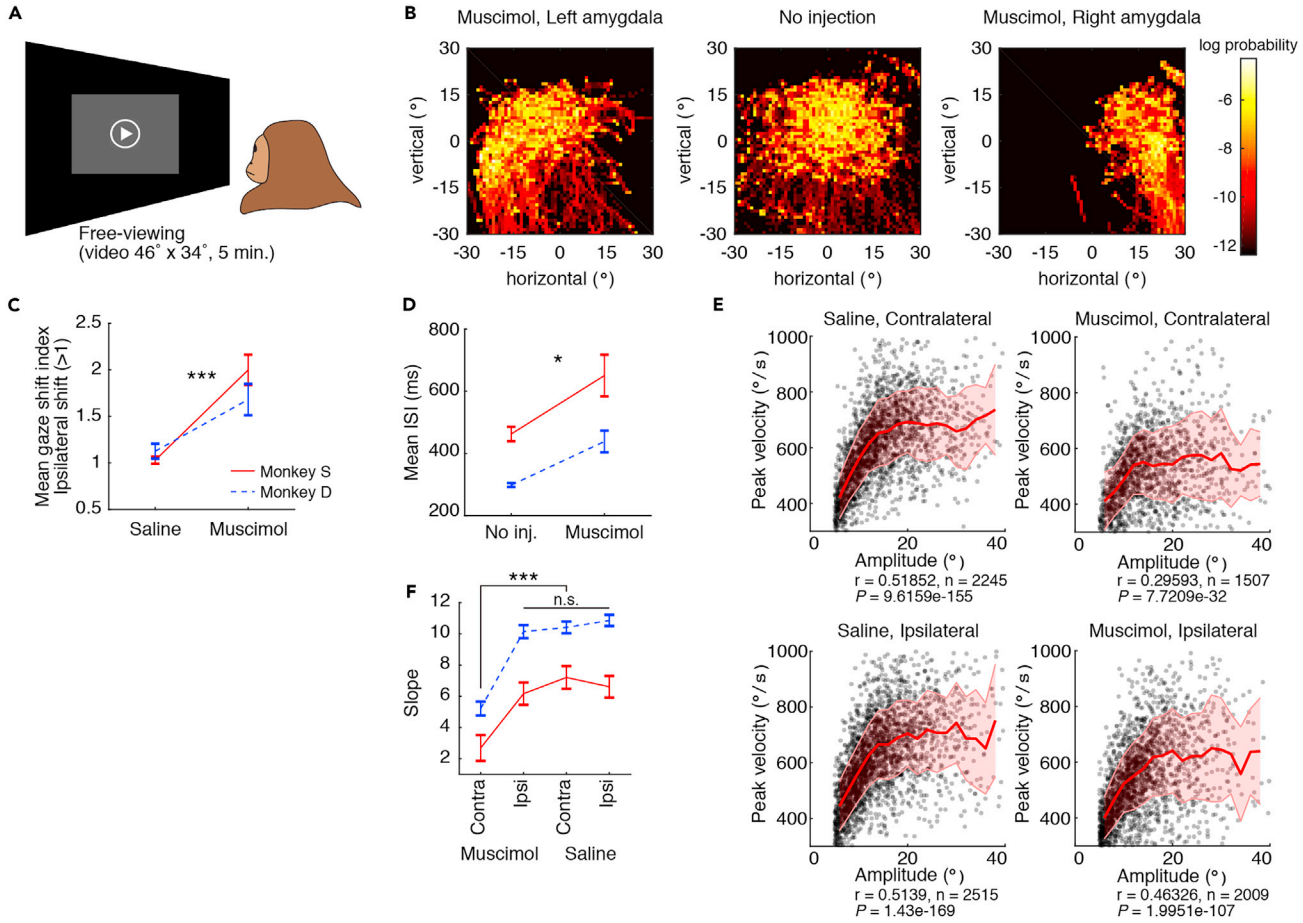

Figure 3. Changes in Free Viewing by Amygdala Inactivation

(A) Free-viewing task.

(B) Gaze positions during a video clip (5 min) in three conditions. The distribution probabilities over time after stimulus onset were calculated by logarithmic two-dimensional histograms of vertical and horizontal gaze directions.

(C) Gaze shifts after saline or muscimol injection in the amygdala. The shift index was calculated in each session (see Methods) and the average is plotted.

(D) Inter-saccade interval (ISI) after no injection or muscimol injection in the amygdala.

(E) Relationship between saccade amplitude (abscissa) and peak velocity (ordinate). Solid lines show the average of peak velocity in each 2-degree bin of saccade amplitude. Shading shows SD (Pearson's correlation).

(F) Slopes of regression lines (ANCOVA and post hoc: least significant difference) for the four groups shown in (E).

Error bars in (C), (D), and (F) show SEM. Asterisks (*) and (***) indicate statistically significant contrasts at $p < 0.05$ and $p < 0.001$. All data in B and E are for monkey D (Figure S4 for monkey S).

(t test, $T(98) = -58.1173$, $p = 9.3491 \times 10^{-78}$). The population activity of 18 neurons recorded is shown in Figure 4B (right).

Moreover, the optical stimulation of the amygdala induced contralateral saccades (Figure 4C) while the monkey was freely viewing. Both monkeys made saccades more frequently to the side contralateral to the stimulation (Figure 4C upper, monkey S; Figure 4C lower, monkey D). This effect started soon after the onset of 200-ms optical stimulation pulses and persisted for at least 400 ms. The contralateral facilitation commonly appeared across sessions and monkeys (Figure 4D, right-tailed one-sample t test, nested data: $p = 0.014391$, monkey S: $p = 0.18396$, monkey D: $p = 0.019764$). These results were complementary to the effect of the muscimol injection, indicating that the amygdala facilitates saccadic eye movements to the contralateral side.

As a control, we assessed the effects of optical stimulation without viral vector expression on the contralateral side in monkey S and in another monkey. Example neurons and saccadic biases are shown in

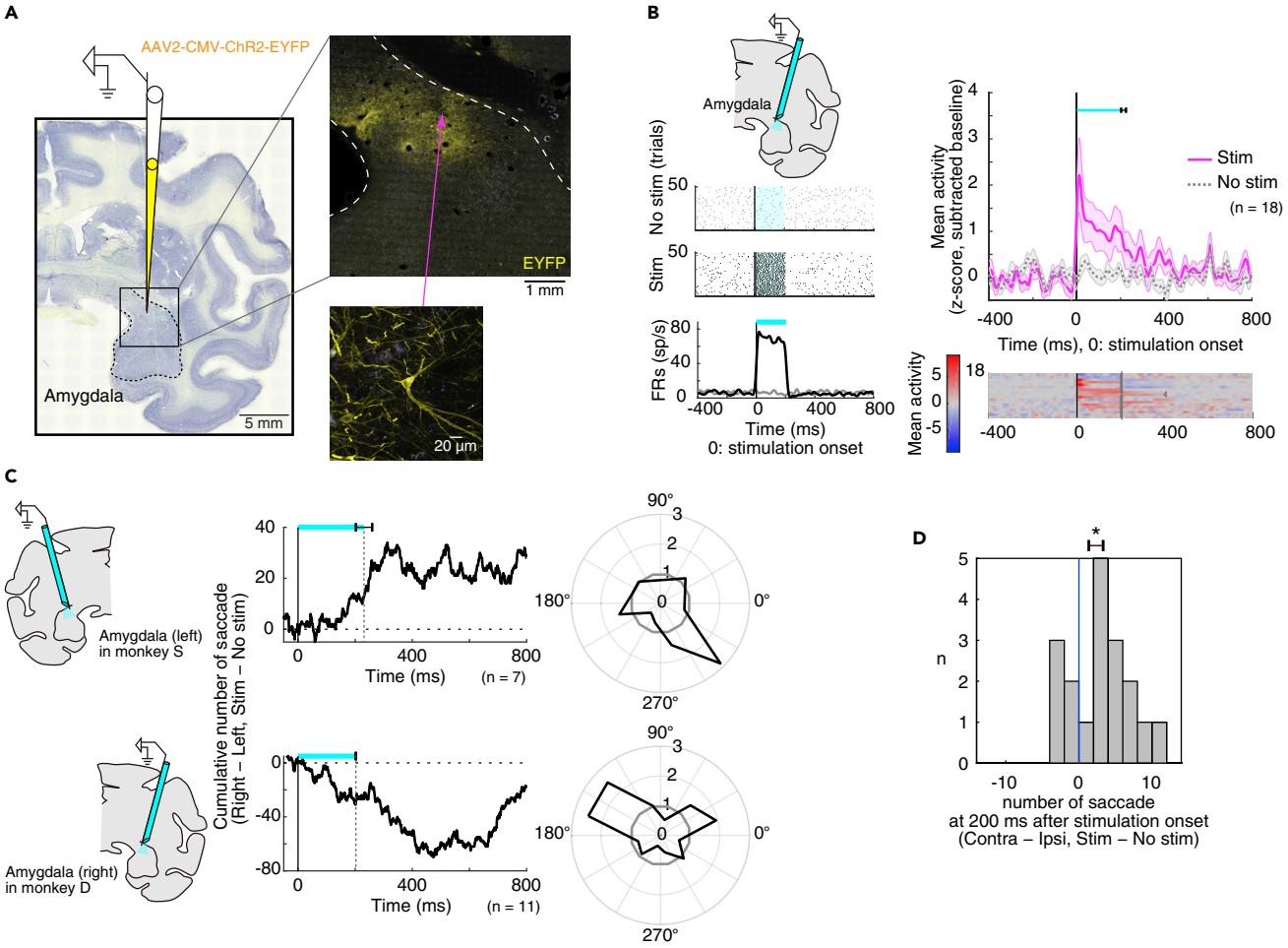

Figure 4. Optogenetic Activation of Amygdala Facilitates Contralateral Saccades

(A) Injection site (left) and AAV2-CMV-ChR2-EYFP infections (right) in the amygdala (yellow: EYFP, blue: autofluorescence). Right-bottom shows EYFP expressions in a cell body of a CeA neuron.

(B) Effects of optical stimulation on amygdala neurons. Left: activity of a CeA neuron around the no-stimulation period (top) and the stimulation period (200 ms) (center). Changes in firing rate in the stimulation/no-stimulation conditions are shown at bottom. Right: activity of 18 amygdala neurons. Population activity is shown at top. Spike activity was smoothed with a Gaussian kernel (σ = 10 ms). The cyan bar shows mean stimulation durations, and the error bar shows SEM. Responses of individual neurons (bottom) were converted to color scale and sorted by modulation latencies. Dots indicate the end of optical stimulation. The duration of optical stimulation was about 200 ms, except for one neuron (400 ms).

(C) Directional bias of saccades by amygdala optical stimulation. In monkey S (upper), stimulation was in the left amygdala and saccades were biased to the right. In monkey D (lower), stimulation was in the right amygdala and saccades were biased to the left. Center: cumulative direction bias, which is aligned on the onset of optical stimulation. Right: polar plot showing ratio of saccades in radial directions in stimulation(+) versus stimulation(−) conditions (bin width = 30 deg). Values greater than 1 indicate more saccades in the stimulation(+) condition.

(D) Bias of the number of saccades during the stimulation to each amygdala neuron (right-tailed one-sample t test). The error bar shows SEM. Asterisk (*) indicates statistically significant contrasts at $p < 0.05$.

Figure S6, which did not exhibit any clear modulation. Thus, the laser light by itself did not affect either neuronal activity or animal's behavior.

Activation of Amygdalo-Nigral Pathway

Having established the efficacy of our viral vector injection, we proceeded to ask what specific circuit is implicated in facilitating contralateral saccades. It has been shown anatomically that CeA projects to SNr (Fudge and Haber, 2000; Gerfen et al., 1982; Price and Amaral, 1981; Shinonaga et al., 1992), which in turn controls saccades through its inhibitory connection to SC (Hikosaka et al., 2000; Hikosaka and Wurtz, 1983). To manipulate this circuit, we used optrodes to test how SNr neurons responded to optical stimulation of axon terminals that originated from the amygdala and expressed ChR2.

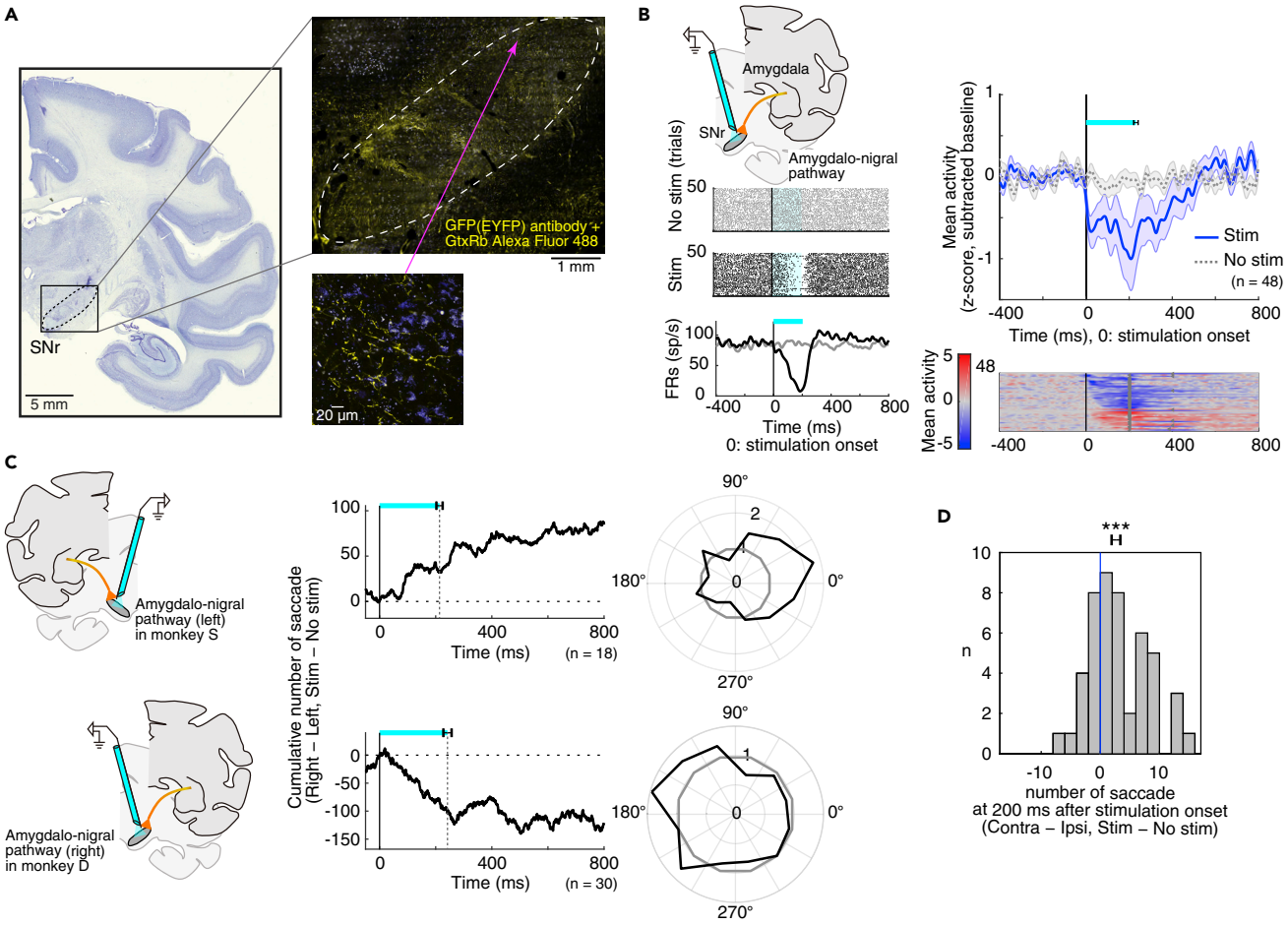

Figure 5. Amygdalo-Nigral Inhibitory Pathway Modulates Oculomotor Behavior

(A) Enhanced anterograde transport of AAV2-CMV-ChR2-EYFP infection in SNr (yellow: GFP(EYFP) antibody + GtxRb Alexa Fluor 488, blue: autofluorescence). Right-bottom shows the expressions in axons.

(B–D) SNr neuronal modulation and directional bias of saccades after optical stimulation of the amygdalo-nigral pathway. Same format as in Figures 4B–4D. (B, right) Activity of 48 SNr neurons that were excited or inhibited by optogenetic stimulation (inhibition: n = 34, excitation: n = 14). (D) Error bars show SEM. Asterisks (***) indicate statistically significant contrasts at $p < 0.001$.

We examined neurons in the wide area of SNr (monkey S, n = 46; monkey D, n = 46), and found that about half of the SNr neurons were affected by optical stimulation (48/92, monkey S: 18, monkey D: 30), suggesting that they received inputs from the amygdala. Figure 5B (left) shows the response of a typical SNr neuron, which was inhibited during the optical stimulation. Most neurons tested were inhibited by the stimulation (n = 34/48, monkey S: 15, monkey D: 19), although some neurons were excited (Figure 5B, right-lower, n = 14/48, monkey S: 3, monkey D: 11). Both groups of neurons were distributed widely in SNr (Figure S5C). On average the population of SNr neurons were inhibited during the optical stimulation, which diminished gradually after the offset of the light pulse (Figure 5B, right-upper). These results suggest that a number of neurons in CeA have direct connections to SNr neurons, predominantly with inhibitory synapses. Indeed, many ChR2-positive axon terminals were found in SNr (Figure 5A).

We found that optical stimulation in SNr induced contralateral saccades in both monkeys (Figure 5C). This contralateral facilitation was significant across sessions (Figure 5D, right-tailed one-sample t test, nested data: $p = 0.0003963$, monkey S: $p = 0.0074748$, monkey D: $p = 0.0067764$). The results were similar to those obtained with the optical stimulation in the amygdala (Figures 4C and 4D). These data together suggest that the amygdala, especially CeA, facilitates contralateral saccades through its inhibitory connection to SNr. According to this model, saccades would be permitted by a disinhibition of SC neurons (Figure 7).

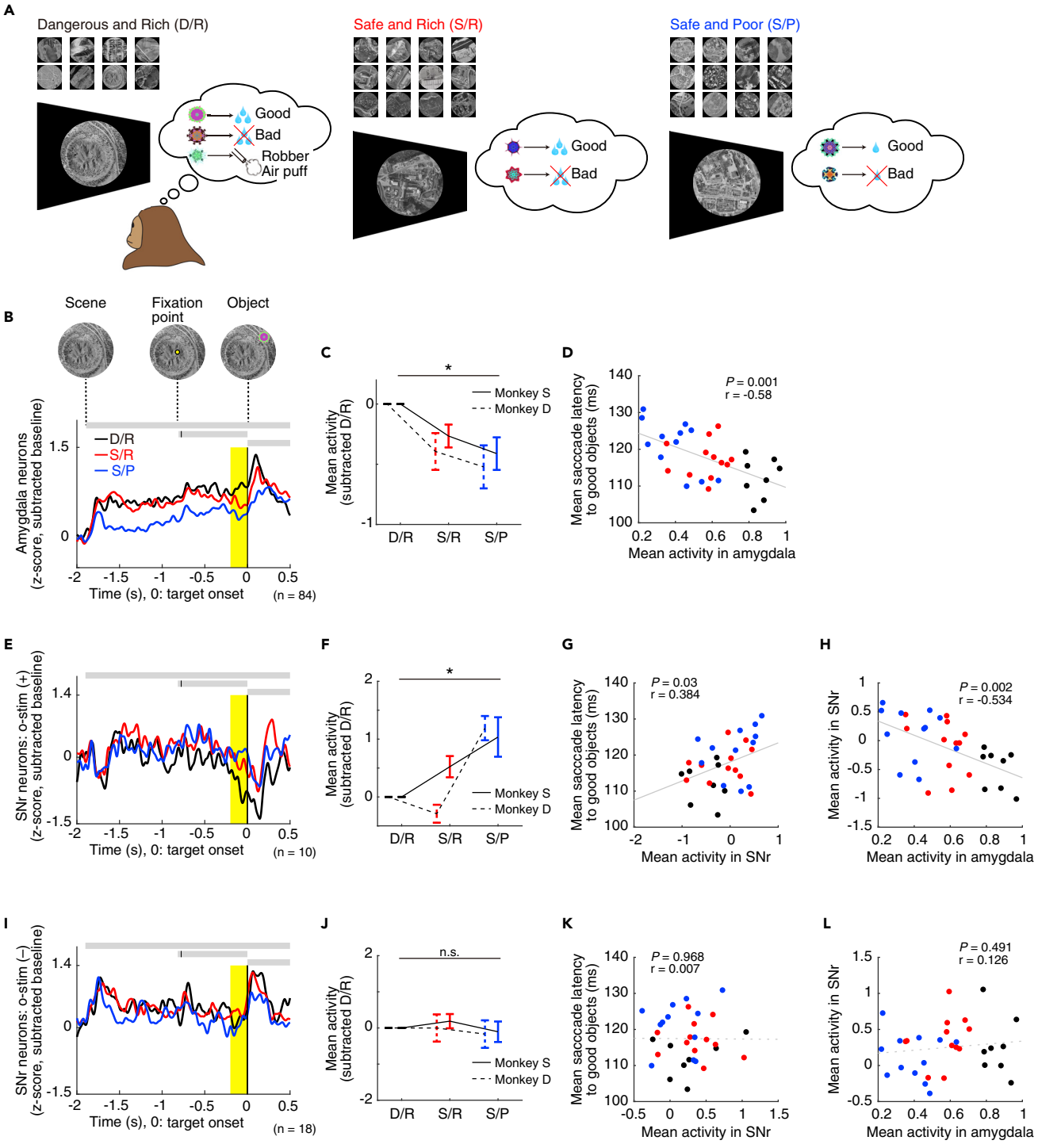

Figure 6. Amygdala Is Excited and SNr Is Inhibited by Motivating Contexts

(A) Foraging task in three different contexts (D/R: 8, S/R: 12, S/P: 12 scenes).

(B–D) Population activity of amygdala neurons (black: D/R, red: S/R, blue: S/P). (B) Activity changes of amygdala neurons during the period including the onsets of scene, fixation point, and object in monkey S. (C) Mean amygdala activity in each context. This was calculated during the period 200 ms before the object onset (shaded yellow area in B). Error bars indicate SEM. (D) Relation between the mean amygdala activity (abscissa) and mean saccade latency (ordinate) (Pearson's correlation) in monkey S. Data are presented separately for individual scenes that are shown in (A).

Figure 6. *Continued*
(E–H) Population activity of SNr neurons that were optogenetically manipulated. E–G, same format as in B–D. (H) Relation between the mean amygdala activity (abscissa) and mean SNr activity (ordinate) for individual scenes (Pearson's correlation).
(I–L) Population activity of SNr neurons that were not optogenetically manipulated. I–K, same format as in B–D. (L) Relation between the mean amygdala activity (abscissa) and mean SNr activity (ordinate) for individual scenes (Pearson's correlation). All neuronal data are for monkey S (Figure S7 for monkey D).

Amygdalo-Nigral Activity in Motivating Contexts

An important question arises as to what type of information is sent from the amygdala to SNr. Data in Figure S3 suggested that the amygdala, especially CeA, does not modulate saccades based on object values, unlike the basal ganglia (Kim and Hikosaka, 2013; Tachibana and Hikosaka, 2012). Using a scene-based foraging task, we previously found that amygdala neurons tended to be activated in motivating contexts (Maeda et al., 2018). Here, we examined activity of amygdala neurons as well as SNr neurons using the same foraging task (Figure 6A).

In each trial of the task, the screen in front of the monkey was dark at first. Next, a large visual scene (chosen from satellite imagery) appeared suddenly, which acted as an environmental context. Each scene contained at least two fractal objects, which appeared one at a time, randomized in both sequence and position. Target objects were associated with either reward (water) or no reward, referred to as "good" and "bad" objects, respectively. A different fractal object called the "robber" could appear in some scenes, which signaled the threat of an air puff and possible cancellation of the reward. The monkeys were rewarded for making saccades to the good objects and holding fixation for 400 ms. The task had three different emotional contexts depending on the objects consistently associated with the scenes (Figure 6A): (1) D/R: dangerous (robber+) and rich (large reward), (2) S/R: safe (robber−) and rich (large reward), and (3) S/P: safe (robber−) and poor (small reward).

Amygdala neurons were most strongly activated with the D/R context, followed by the S/R and then the S/P context (Figures 6B, 6C, and S7C). Across all scenes tested, stronger neuronal responses were associated with shorter saccade latencies (Figures 6D and S7D). At the same time, neuronal activity was positively correlated with mean heart rate in each scene (Figure S7A), consistent with the expectation that amygdala activation was linked to emotional arousal. These data suggest that the emotional (i.e., motivating) contexts activate amygdala neurons, which then initiates saccades earlier.

The results from our optogenetic activation of axon terminals showed that the inhibitory connection from the amygdala to the SNr facilitated contralateral saccades (Figure 5). We therefore asked whether this neural pathway accounts for the modulation of saccades in emotional contexts. To address this question, we tested two groups of SNr neurons using the scene-based foraging task: (1) O-stim (+) neurons (i.e., activity affected by optogenetic stimulation; n = 17, monkey S: 10, monkey D: 7) (Figures 6E–6H and S7E–S7G); (2) O-stim (−) neurons (i.e., unaffected by optogenetic stimulation; n = 25, monkey S: 18, monkey D: 7) (Figures 6I–6L and S7H–S7J).

O-stim (+) SNr neurons, which were likely to receive direct inputs from the amygdala, were more strongly inhibited with the D/R or S/R context than with the S/P context in the absence of optical stimulation (Figures 6E, 6F, S7E). Moreover, lower activity of these neurons was associated with shorter saccadic latencies (Figure 6G and S7F). Finally, the activity changes across many scenes were negatively correlated between amygdala neurons and O-stim (+) SNr neurons (Figure 6H and S7G). In contrast, O-stim (−) SNr neurons, which were less likely to receive direct inputs from the amygdala, showed none of these effects: not modulated by contextual information (Figures 6I, 6J, and S7H) and not related to the saccade latencies and amygdala activities (Figures 6K, 6L, S7, and S7J).

These results reveal a neural circuit mechanism (amygdala-SNr-SC) that boosts the choice of good objects (by saccades) based on the motivational contexts (i.e., dangerous and rich) (Figure 7). Importantly, this mechanism is spatially selective (i.e., contralateral saccades), as required for the choice of one good object among competing alternative objects.

DISCUSSION

Our study defines a possible role of the amygdala in spatially selective oculomotor control based on contextual information. Central to this process is an amygdalo-nigral pathway that inhibits activity of

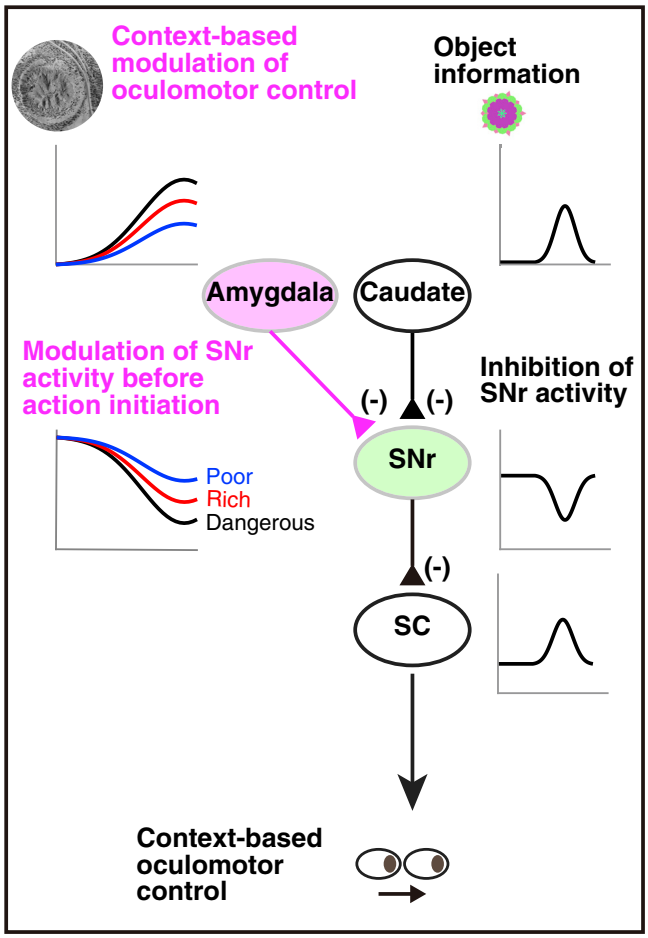

Figure 7. Hypothetical Neural Circuit

SNr, substantia nigra pars reticulata; SC, superior colliculus.

SNr neurons (see Figure 7), contributing to disinhibition of SC neurons to generate saccades (Hikosaka and Wurtz, 1983). Consistent with this result, our pharmacological inactivation data showed that the amygdala inactivation suppressed saccades physically and motivationally (see Figures 1 and 2). Previous studies have revealed that neurons in the striatum (caudate nucleus and putamen) respond to many visual objects phasically and also encode the historical values of objects (Kim and Hikosaka, 2013; Kunimatsu et al., 2019; Yamamoto et al., 2013). The striatal neurons that have GABAergic (γ-aminobutyric-acid-releasing) projections to SNr control oculomotor behaviors based on the object information (Hikosaka et al., 2000; Yasuda et al., 2012). In the current findings, it is important to note that tonic activity of SNr neurons is modulated by emotional and motivational contexts (i.e., dangerous versus safe, rich versus poor) before object appearance and that the SNr neurons receive input from CeA encoding contextual information. These findings suggest that two different aspects of oculomotor control, pertaining to context and object, are mediated by distinct inhibitory inputs to SNr from the amygdala and striatum, respectively (see Figure 7).

Together with our previous findings (Maeda et al., 2018, 2019), these results suggest that the amygdala governs social and emotional behaviors at multiple levels. At the most general level, the amygdala mediates context-appropriate social orienting, as evidenced by the effect of amygdala inactivation during movie free viewing (Maeda et al., 2019). At a more fine-grained level, the amygdala selectively mediates the spatially oriented action required for finding objects of interest quickly and accurately. This goal-directed aspect of amygdala function was disrupted by amygdala inactivation and facilitated by optogenetic activation of the amygdala or the amygdalo-nigral pathway. Both levels must work in tandem for appropriate behavior to take place, as the general promotion of a context-appropriate behavioral regimen must be followed by narrowly targeted actions aimed at choosing or rejecting particular objects. To this end behavior must be controlled accurately, especially in the

spatial domain, otherwise random involuntary movements would prevail. For this reason, the spatially selective (i.e., contralateral) control of saccades by the amygdala is critical.

These data are relevant to the neural circuit concept proposed by Swanson and Petrovich (Swanson and Petrovich, 1998) that CeA in the rat is a region of the striatum specialized to modulate the autonomic motor outflow by inhibitory signals. In the monkey, CeA modulates goal-directed action (i.e., saccade and gaze) (see Figures 1, 2, 3, 4, and 5), possibly in addition to autonomic actions including the heart rate (see Figure S7A) and pupil size (see Figure 7 in a previous article (Maeda et al., 2018)). A recent study on the mouse revealed that CeA preferentially inhibited GABAergic neurons in the lateral substantia nigra, which corresponds to the lateral part of SNr in the monkey (Francois et al., 1984), and the circuit modulated emotional responses to salient stimuli (Steinberg et al., 2020). Such a coordination of autonomic and voluntary motor actions is crucial for responding appropriately to a given emotional/motivational context, which is utilized commonly in different animals.

These data suggest that the basal ganglia output can be modulated by other brain areas for goal-directed behavior. The final stage of the basal ganglia circuit, namely the SNr-SC pathway, has connection patterns well suited for promoting appropriate choices (Hikosaka et al., 2000): widespread inhibition of many unnecessary objects/actions and selective disinhibition of necessary objects/actions. Accordingly, brain areas outside the basal ganglia could participate in goal-directed behavior by sending inhibitory signals to SNr neurons, as the amygdala (especially CeA) does. Importantly, this same mechanism can be activated by different sources of information (e.g., object by striatum versus context by CeA). Our data, however, do not exclude the possibility that CeA may also use other targets (e.g., brainstem nuclei (Price and Amaral, 1981)) to control behaviors based on contexts.

A growing body of evidence suggests that the emotional or motivational information in the amygdala affects basal ganglia circuitry, and this modulation is critical for adjusting spatially selective oculomotor behaviors or attention in particular contextual environments. Dysregulation of the amygdala-basal ganglia linkage may contribute to psychiatric conditions, among which adjustment disorders in stressful environments are the most prevalent (Bachem and Casey, 2018; Zelviene and Kazlauskas, 2018). Interestingly, a recent study has shown that bilateral sensory stimulation reduces traumatic memory and facilitates adaptation to stressful environments by modulating a multisynaptic SC-mediodorsal thalamus-amygdala pathway (Baek et al., 2019). In humans, treatment regimens have been developed to utilize eye movements against stress disorders (i.e., eye movement desensitization and reprocessing) (Shapiro, 2001). Our present study defines that the amygdalo-nigral pathway in primates controls saccadic eye movements in stressful environments (or, motivating contexts) and that its dysfunction leads to behavioral impairments. A more precise functional understanding of this pathway will provide new insights into the possible mechanism underlying human psychiatric symptoms associated with adjustment disorders.

Limitations of the Study

- This study shows the inhibitory effects of the amygdala on SNr neurons, which facilitates saccades to the contralateral side. However, there might be other effects of the amygdala on the basal ganglia that may be mediated by the connections to the striatum or GPe.
- We focused on the central nucleus of the amygdala but have not examined the amygdala as a whole. This could be tested by injecting viral vector in other amygdala nuclei.
- The optogenetic stimulation was performed with the single-unit electrophysiological recording, which may overlook the effect on neuronal circuits in SNr. This may be solved by multi-unit recording methods.

Resource Availability

Lead Contact

Further information and requests for resources should be directed to and will be fulfilled by the Lead Contact, Kazutaka Maeda (kaz.maeda.86@gmail.com).

Materials Availability

Materials and the information used for the experiments are available upon reasonable request.

Data and Code Availability

Original data have been deposited to Mendeley Data: [https://doi.org/10.17632/g2shdsbtgt.1].

METHODS

All methods can be found in the accompanying Transparent Methods supplemental file.

SUPPLEMENTAL INFORMATION

Supplemental Information can be found online at https://doi.org/10.1016/j.isci.2020.101194.

ACKNOWLEDGMENTS

We thank H. Amita for assistance with optogenetic experiments; D. McMahon for manuscript-writing assistance; NEI Biological Imaging Core Facility and A Gopal for assistance with confocal microscopy; and M.K. Smith, D. Parker, D. O'Brien, V.L. McLean, I. Bunea, G. Tansey, D. Yu, A.M. Nichols, T. W. Ruffner, J.W. McClurkin, J. Fuller-Deets, and A.V. Hays, and M Fujiwara for technical assistance. This work was supported by Intramural Research Program at the National Eye Institute, the National Institutes of Health, United States (project number: 1ZIAEY000415-16, https://projectreporter.nih.gov/project_info_details.cfm?aid=9796699&map=y), the Japan Agency for Medical Research and Development, Japan (Grants JP18dm0307021 and JP18dm0207003), and the Japan Science and Technology Agency, Japan (PRESTO Grant JPMJPR1683).

AUTHOR CONTRIBUTIONS

K.M. and O.H. designed this research, performed the experiments, analyzed the data, and wrote the manuscript. K.I. and M.T. produced the viral vector. K.M., K.I., J.K., M.T., and O.H. discussed the results.

DECLARATION OF INTERESTS

The authors declare no competing financial interests.

Received: January 10, 2020
Revised: April 12, 2020
Accepted: May 19, 2020
Published: June 26, 2020

REFERENCES

Amita, H., Kim, H.F., Smith, M., Gopal, A., and Hikosaka, O. (2019). Neuronal connections of direct and indirect pathways for stable value memory in caudal basal ganglia. Eur. J. Neurosci. *49*, 712–725.

Avino, T.A., Barger, N., Vargas, M.V., Carlson, E.L., Amaral, D.G., Bauman, M.D., and Schumann, C.M. (2018). Neuron numbers increase in the human amygdala from birth to adulthood, but not in autism. Proc. Natl. Acad. Sci. U S A *115*, 3710–3715.

Bachem, R., and Casey, P. (2018). Adjustment disorder: a diagnosis whose time has come. J. Affective Disord. *227*, 243–253.

Baek, J., Lee, S., Cho, T., Kim, S.-W., Kim, M., Yoon, Y., Kim, K.K., Byun, J., Kim, S.J., Jeong, J., et al. (2019). Neural circuits underlying a psychotherapeutic regimen for fear disorders. Nature *566*, 339–343.

Baloh, R.W., Sills, A.W., Kumley, W.E., and Honrubia, V. (1975). Quantitative measurement of saccade amplitude, duration, and velocity. Neurology *25*, 1065–1070.

Behrmann, M., Watt, S., Black, S.E., and Barton, J.J. (1997). Impaired visual search in patients with unilateral neglect: an oculographic analysis. Neuropsychologia *35*, 1445–1458.

Constantino, J.N., Kennon-McGill, S., Weichselbaum, C., Marrus, N., Haider, A., Glowinski, A.L., Gillespie, S., Klaiman, C., Klin, A., and Jones, W. (2017). Infant viewing of social scenes is under genetic control and is atypical in autism. Nature *547*, 340–344.

Corbetta, M., Akbudak, E., Conturo, T.E., Snyder, A.Z., Ollinger, J.M., Drury, H.A., Linenweber, M.R., Petersen, S.E., Raichle, M.E., Van Essen, D.C., et al. (1998). A common network of functional areas for attention and eye movements. Neuron *21*, 761–773.

Corbetta, M., and Shulman, G.L. (2002). Control of goal-directed and stimulus-driven attention in the brain. Nat. Rev. Neurosci. *3*, 201–215.

Dal Monte, O., Costa, V.D., Noble, P.L., Murray, E.A., and Averbeck, B.B. (2015). Amygdala lesions in rhesus macaques decrease attention to threat. Nat. Commun. *6*, 10161.

Davis, M., and Whalen, P.J. (2001). The amygdala: vigilance and emotion. Mol. Psychiatry *6*, 13–34.

Francois, C., Percheron, G., and Yelnik, J. (1984). Localization of nigrostriatal, nigrothalamic and nigrotectal neurons in ventricular coordinates in macaques. Neuroscience *13*, 61–76.

Fudge, J.L., and Haber, S.N. (2000). The central nucleus of the amygdala projection to dopamine subpopulations in primates. Neuroscience *97*, 479–494.

Gerfen, C.R., Staines, W.A., Arbuthnott, G.W., and Fibiger, H.C. (1982). Crossed connections of the substantia nigra in the rat. J. Comp. Neurol. *207*, 283–303.

Griggs, W.S., Kim, H.F., Ghazizadeh, A., Gabriela Costello, M., Wall, K.M., and Hikosaka, O. (2017). Flexible and stable value coding areas in caudate head and tail receive anatomically distinct cortical and subcortical inputs. Front. Neuroanat. *11*, 106.

Hikosaka, O., Takikawa, Y., and Kawagoe, R. (2000). Role of the basal ganglia in the control of purposive saccadic eye movements. Physiol. Rev. *80*, 953–978.

Hikosaka, O., and Wurtz, R.H. (1983). Visual and oculomotor functions of monkey substantia nigra pars reticulata. IV. Relation of substantia nigra to superior colliculus. J. Neurophysiol. *49*, 1285–1301.

Hikosaka, O., and Wurtz, R.H. (1985a). Modification of saccadic eye movements by GABA-related substances. I. Effect of muscimol and bicuculline in the monkey superior colliculus. J. Neurophysiol. *53*, 266–291.

Hikosaka, O., and Wurtz, R.H. (1985b). Modification of saccadic eye movements by GABA-related substances. II. Effects of muscimol in monkey substantia nigra pars reticulata. J. Neurophysiol. *53*, 292–308.

Hoffman, J.E., and Subramaniam, B. (1995). The role of visual attention in saccadic eye movements. Percept Psychophys *57*, 787–795.

Kim, H.F., and Hikosaka, O. (2013). Distinct basal ganglia circuits controlling behaviors guided by flexible and stable values. Neuron *79*, 1001–1010.

Kunimatsu, J., Maeda, K., and Hikosaka, O. (2019). The caudal part of putamen represents the historical object value information. J. Neurosci. *39*, 1709–1719.

Maeda, K., Inoue, K.-i., Kunimatsu, J., Takada, M., and Hikosaka, O. (2019). Amygdala controls saccade and gaze physically, motivationally, and socially. bioRxiv, 608703.

Maeda, K., Kunimatsu, J., and Hikosaka, O. (2018). Amygdala activity for the modulation of goal-directed behavior in emotional contexts. Plos Biol. *16*, e2005339.

Miyashita, N., Hikosaka, O., and Kato, M. (1995). Visual hemineglect induced by unilateral striatal dopamine deficiency in monkeys. Neuroreport *6*, 1257–1260.

Munoz, D.P., Armstrong, I.T., Hampton, K.A., and Moore, K.D. (2003). Altered control of visual fixation and saccadic eye movements in attention-deficit hyperactivity disorder. J. Neurophysiol. *90*, 503–514.

Peck, C.J., and Salzman, C.D. (2014). Amygdala neural activity reflects spatial attention towards stimuli promising reward or threatening punishment. Elife *3*, e04478.

Price, J.L., and Amaral, D.G. (1981). An autoradiographic study of the projections of the central nucleus of the monkey amygdala. J. Neurosci. *1*, 1242–1259.

Robinson, D.A. (1964). The mechanics of human saccadic eye movement. J. Physiol. *174*, 245–264.

Shapiro, F. (2001). Eye Movement Desensitization and Reprocessing (EMDR), Second Edition (Guilford Press).

Shinonaga, Y., Takada, M., and Mizuno, N. (1992). Direct projections from the central amygdaloid nucleus to the globus pallidus and substantia nigra in the cat. Neuroscience, 691–703.

Steinberg, E.E., Gore, F., Heifets, B.D., Taylor, M.D., Norville, Z.C., Beier, K.T., Földy, C., Lerner, T.N., Luo, L., Deisseroth, K., and Malenka, R.C. (2020). Amygdala-midbrain connections modulate appetitive and aversive learning. Neuron. https://doi.org/10.1016/j.neuron.2020.03.016.

Swanson, L.W., and Petrovich, G.D. (1998). What is the amygdala? Trends Neurosciences *21*, 323–331.

Tachibana, Y., and Hikosaka, O. (2012). The primate ventral pallidum encodes expected reward value and regulates motor action. Neuron *76*, 826–837.

Taubert, J., Flessert, M., Wardle, S.G., Basile, B.M., Murphy, A.P., Murray, E.A., and Ungerleider, L.G. (2018). Amygdala lesions eliminate viewing preferences for faces in rhesus monkeys. Proc. Natl. Acad. Sci. U S A *115*, 8043–8048.

Vankova, M., Arluison, M., Leviel, V., and Tramu, G. (1992). Afferent connections of the rat substantia nigra pars lateralis with special reference to peptide-containing neurons of the amygdalo-nigral pathway. J. Chem. Neuroanat. 39–50.

Yamamoto, S., Kim, H.F., and Hikosaka, O. (2013). Reward value-contingent changes of visual responses in the primate caudate tail associated with a visuomotor skill. J. Neurosci. *33*, 11227–11238.

Yasuda, M., Yamamoto, S., and Hikosaka, O. (2012). Robust representation of stable object values in the oculomotor Basal Ganglia. J. Neurosci. *32*, 16917–16932.

Yep, R., Soncin, S., Brien, D.C., Coe, B.C., Marin, A., and Munoz, D.P. (2018). Using an emotional saccade task to characterize executive functioning and emotion processing in attention-deficit hyperactivity disorder and bipolar disorder. Brain Cogn. *124*, 1–13.

Zelviene, P., and Kazlauskas, E. (2018). Adjustment disorder: current perspectives. Neuropsychiatr. Dis. Treat. *14*, 375–381.

iScience, Volume *23*

Supplemental Information

Primate Amygdalo-Nigral Pathway for Boosting Oculomotor Action in Motivating Situations

Kazutaka Maeda, Ken-ichi Inoue, Jun Kunimatsu, Masahiko Takada, and Okihide Hikosaka

Supplementary Figures

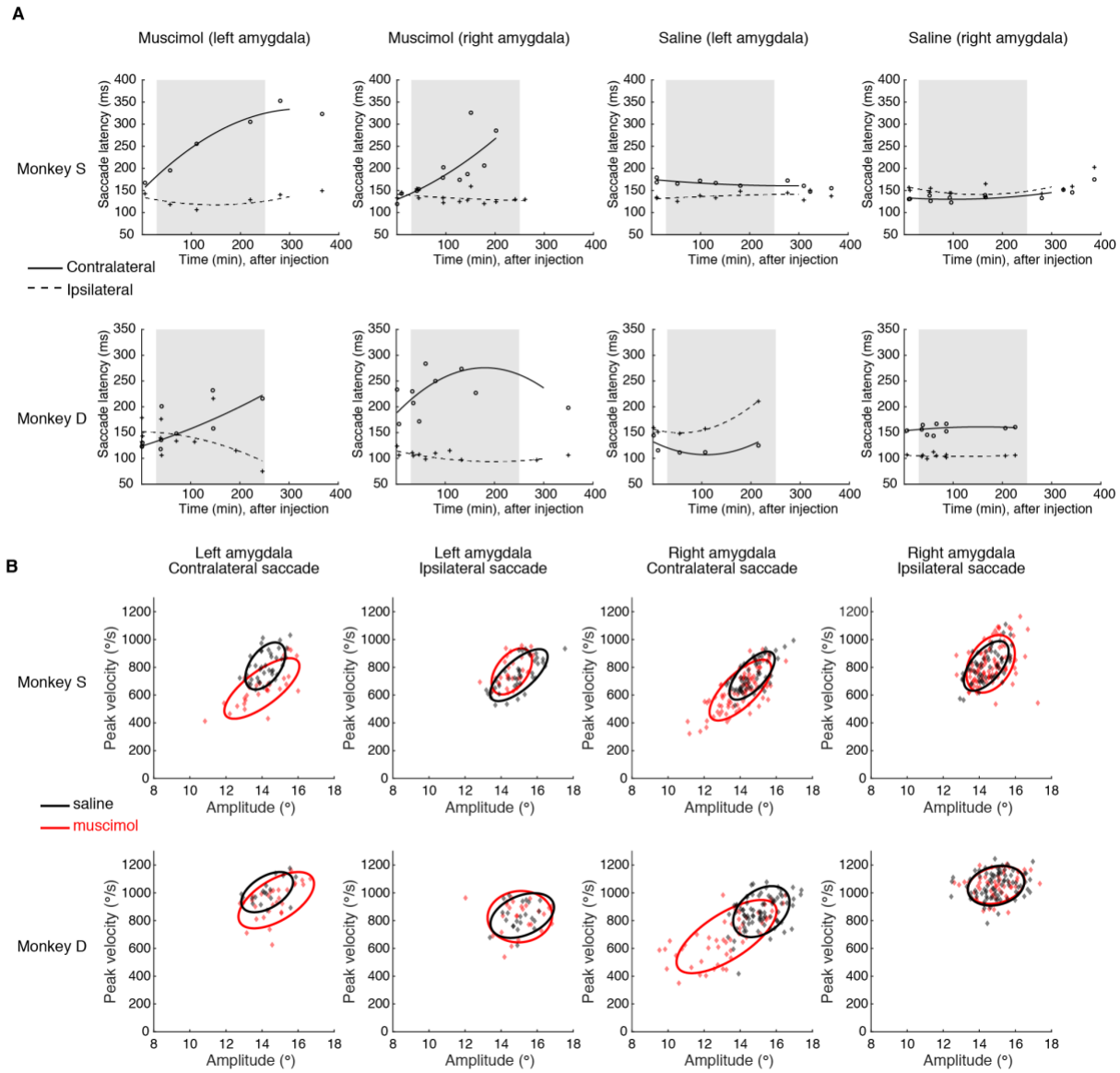

Figure S1. Change in saccade latency, amplitude, and peak velocity following amygdala inactivation (related to Figure 1).
A, Original data of Figure 1D (monkey S) and data from another subject (monkey D) **B**, Original data of Figure 1F (monkey S) and data from another subject (monkey D).

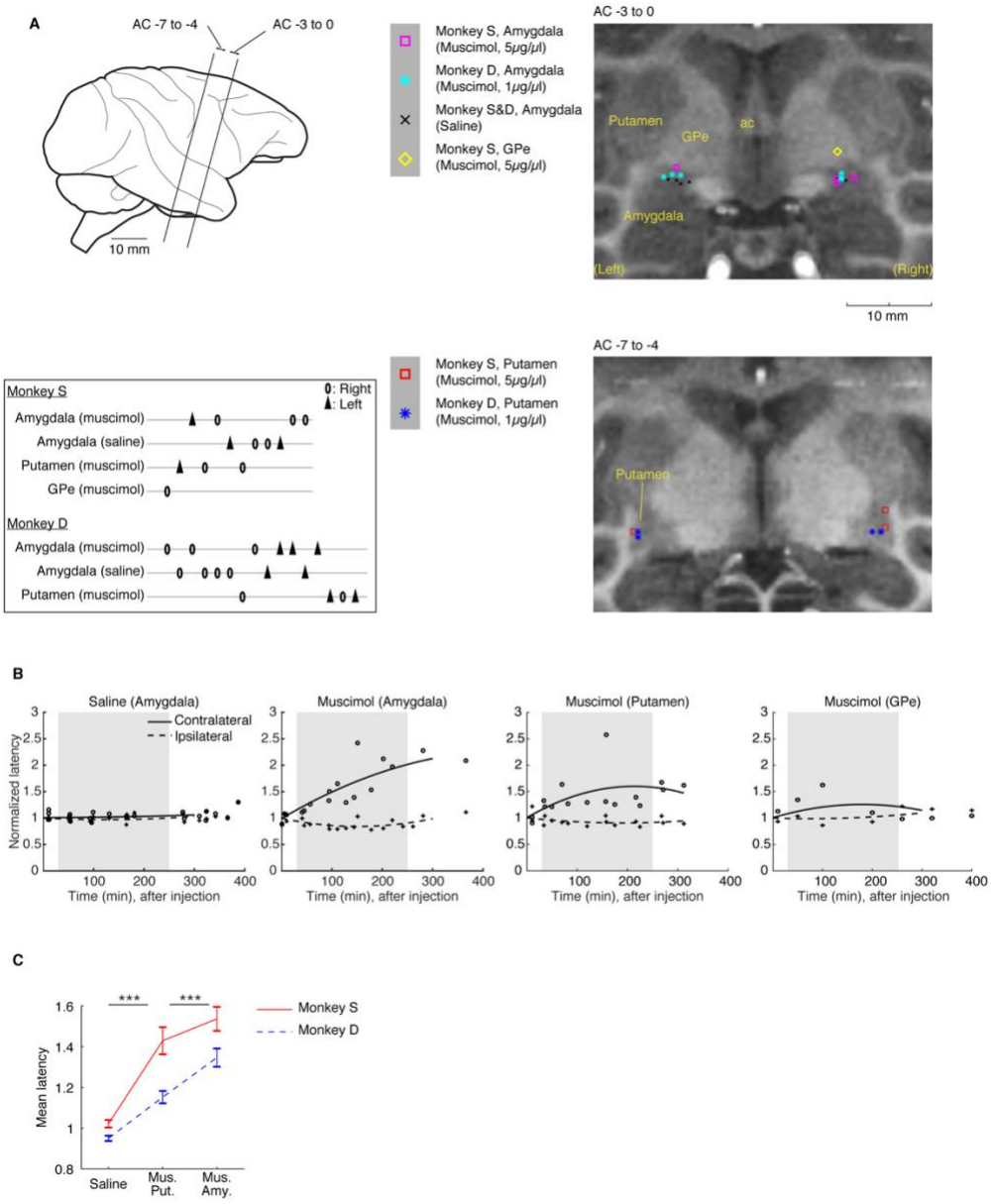

Figure S2. Change in saccade latency following inactivation of the amygdala and surrounding areas (related to Figure 1).

A, Estimated injection sites in the amygdala, GPe, and the putamen. The sites are shown in merged coronal MR images spanning 0-3 mm posterior (top) and 4-7 mm posterior (bottom) to the anterior commissure. ac, anterior commissure. The order of the injections in each monkey is shown in the left-bottom panel (from left to right). **B**, Changes in saccade latency after injection of saline into the amygdala, muscimol into the amygdala, the putamen, and GPe (Data from monkey S). Same format as Figure 1d. **C**, Mean saccade latencies for three conditions (saline injection into the amygdala, muscimol injection into the putamen, and muscimol injection into the amygdala). The individual data point shows the mean latency in each monkey and each condition (red solid line: monkey S, blue dash line: monkey D). Error bar shows SEM. Asterisk (***) indicates statistically significant contrasts at $P < 0.001$ for nested data from both monkeys (one-way ANOVA, post hoc: Fisher's LSD).

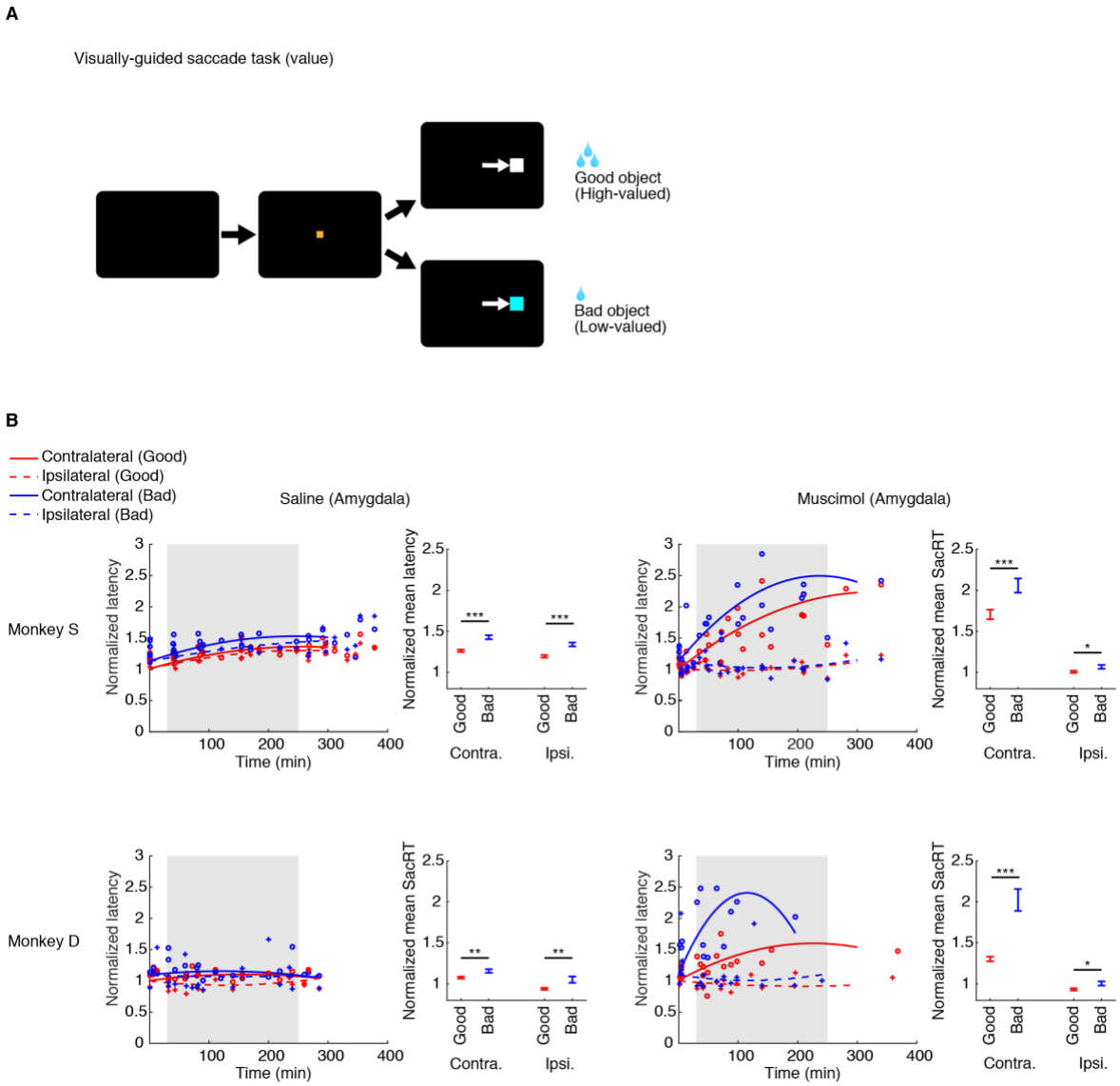

Figure S3. Change in saccade latency to objects of different values following amygdala inactivation (related to Figure 1).
A, Visually-guided saccade task, with target values differing across trials. The white dot (good object) was associated with high reward amount, and the cyan dot (bad object) was associated with low reward amount. **B**, Change in saccade latency by inactivation of the amygdala. Same format as Figure 1D. Asterisks (*), (**), and (***) indicate statistically significant contrasts at $P < 0.05$, $P < 0.01$, and $P < 0.001$ (two-sample t-test).

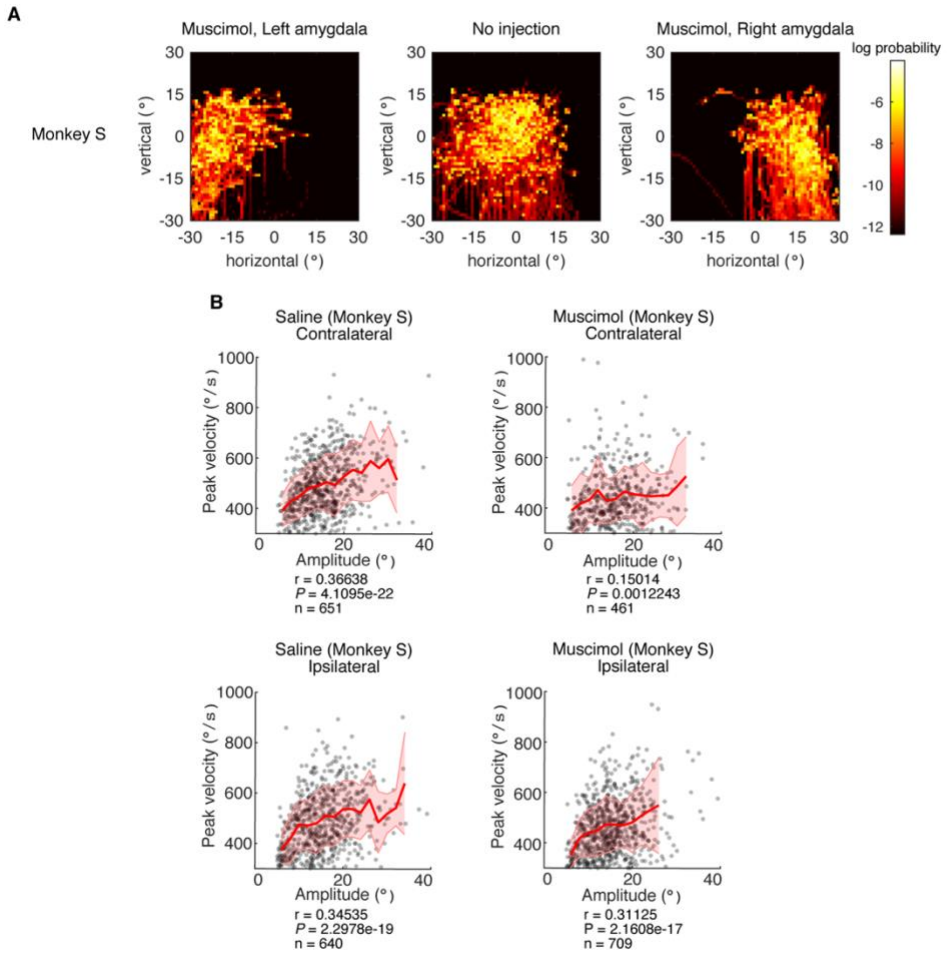

Figure S4. Changes in free viewing following amygdala inactivation (related to Figure 3). **A**-**B**, Data from another subject (monkey S, same format as in Figure 3B and E).

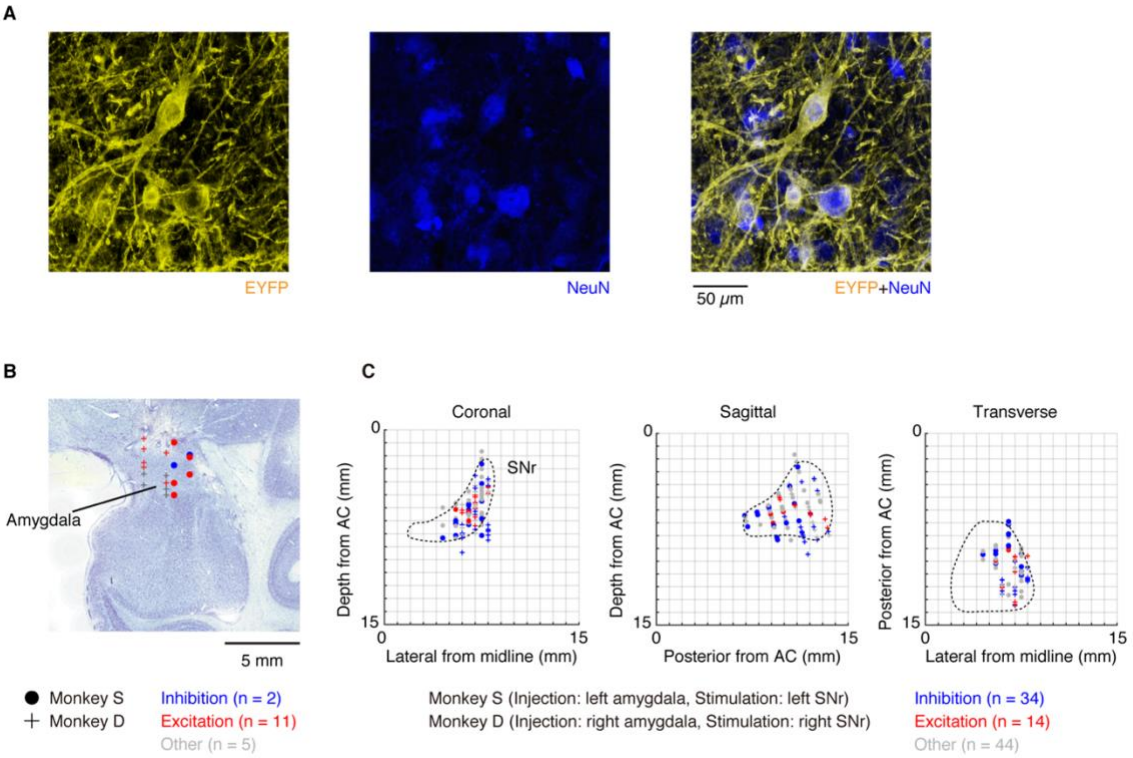

Figure S5. Optogenetic stimulation sites in the amygdala and SNr (related to Figure 4 and Figure 5).

A, Enhanced AAV2-CMV-ChR2-EYFP infection in the amygdala are shown in yellow (left). NeuN-expressing amygdala neurons are shown in blue (middle). Both are shown in the right panel. **B**, Stimulation sites in the amygdala. **C**, Estimated stimulation sites in the SNr.

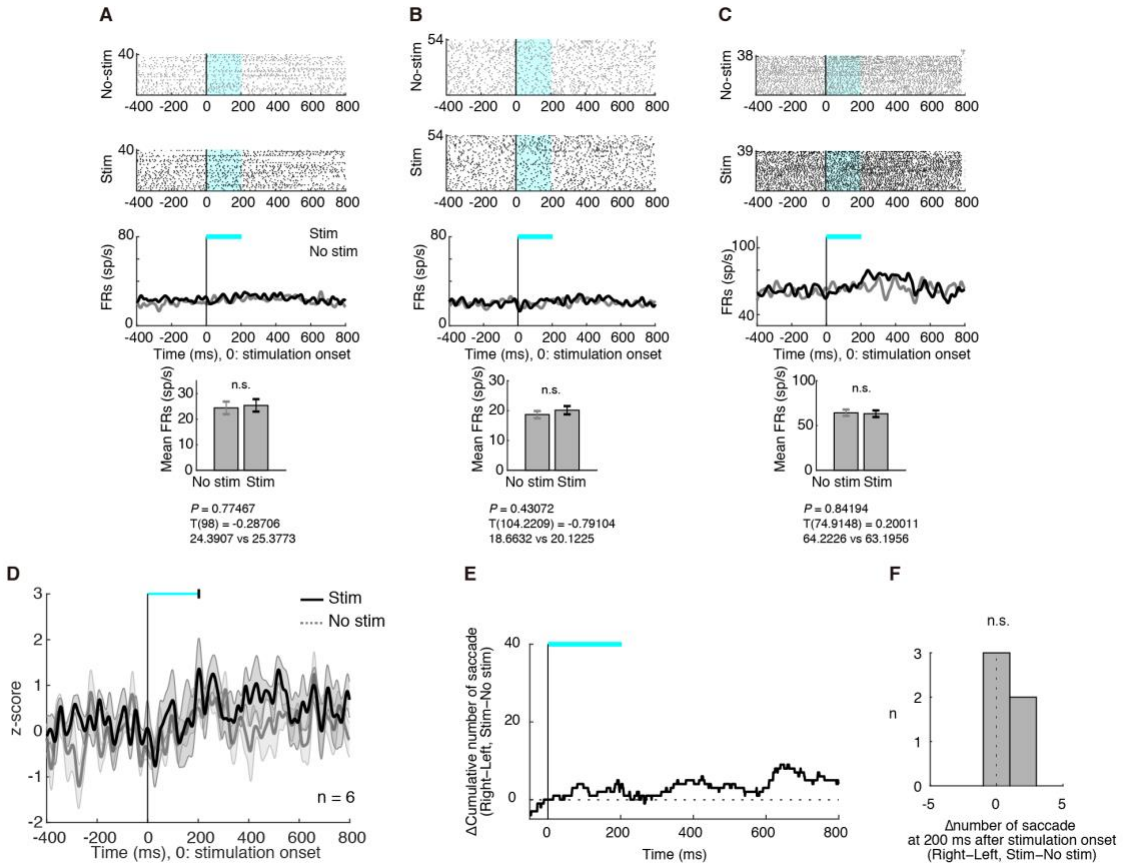

Figure S6. Control data for optogenetic stimulation (related to Figure 4 and Figure 5).
A, Optical stimulation to an example amygdala neuron in another subject (monkey T) without viral expressions. **B**, Optical stimulation of an example amygdala neuron of the right (contralateral) side in monkey S. **C**, Optical stimulation of an example SNr neuron of the right (contralateral) side in monkey S. **D**, Population activity by stimulation in monkey T. Stimulation did not lead to any clear modulation (two sample t-test, T(7.2962) = -0.44275, *P* = 0.67078). The error bars show SEM. **E**, Directional bias of saccades after right (contralateral) amygdala optical stimulation (n = 5) in monkey S. Same format as Figure 4C. **F**, Bias in the number of saccades during the stimulation of the right (contralateral) hemisphere (one-sample t-test, T(4) = 1.5, *P* = 0.104). Same format as Figure 4D.

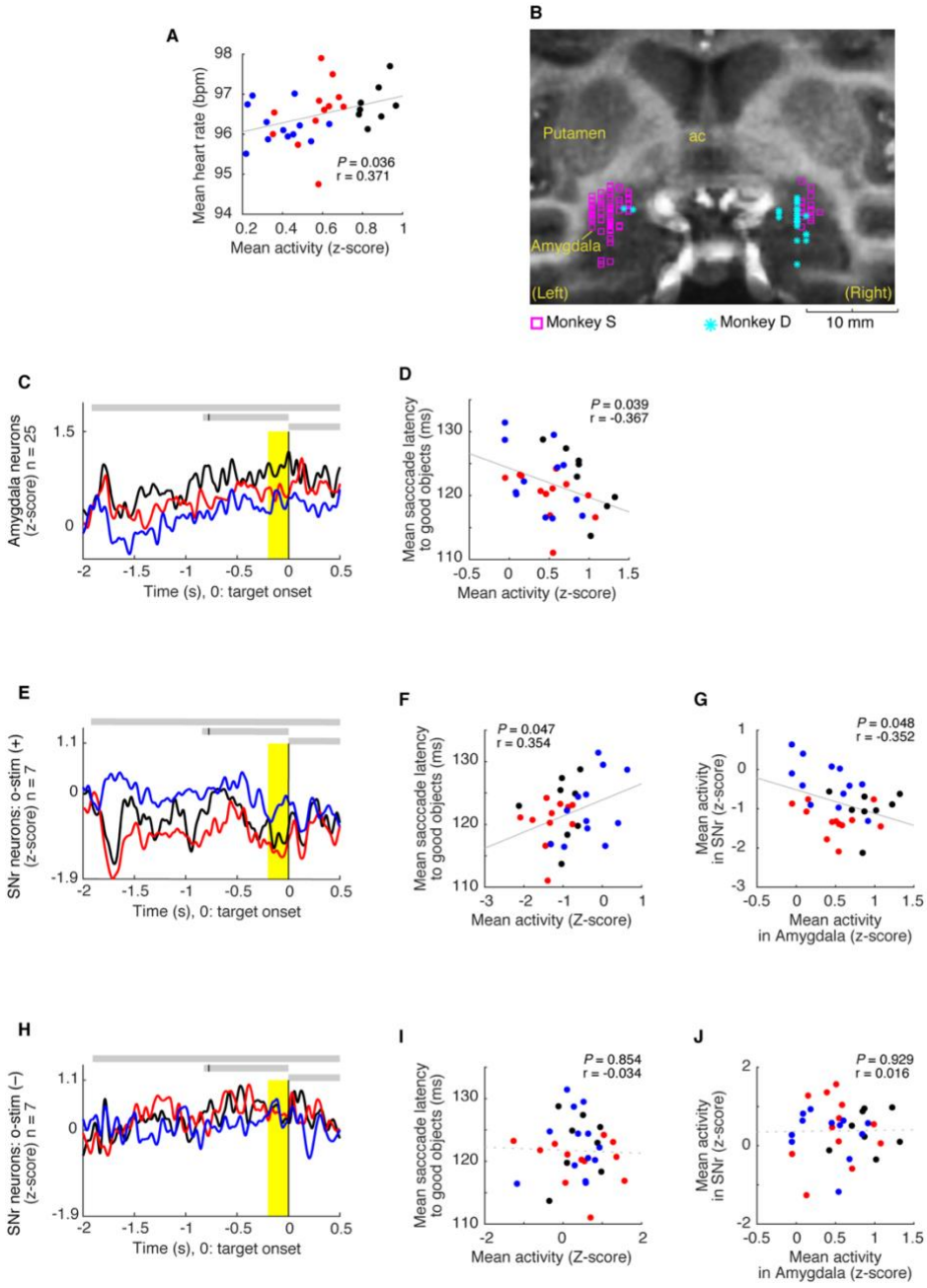

Figure S7. Recording of amygdala and SNr neurons (related to Figure 6).
A, Relation between the mean activity (abscissa) and mean heart rate (ordinate) for individual scenes (Pearson's correlation) in monkey S. **B**, Estimated recording positions. The sites are shown in merged coronal MR images spanning 0-3 mm posterior to the anterior commissure (n = 84 in monkey S, n = 25 in monkey D). ac, anterior commissure. **C**-**J**, Data from monkey D (same format as in Figure 6**B**, **D**, **E**, **G**, **H**, **I**, **K**, and **L**). **C-D**, Population activity of amygdala neurons. **E-G**, Population activity of SNr neurons that were optogenetically manipulated cells. **H-J**, Population activity of SNr neurons that were not optogenetically manipulated cells.

Supplementary Tables

Table S1 (related to Figure 1)

Detail of muscimol injection experiments for the amygdala (task VS: visually-guided saccade, task FV: free-viewing task, Mus.: muscimol). AC: anterior commissure. The positions listed below are chamber coordinates, which were tilted 15 degrees anteriorly relative to the stereotaxic reference frame (millimeter).

Monkey	Concn., µg/µl	Volume (µl)	Injection side	Posterior from AC (mm)	Lateral from midline (mm)	Depth from AC (mm)	Tasks
D	Mus. 1µg/µl	1	Left	2	9	5.9	VS, FV
D	Mus. 1µg/µl	1	Left	3	11	6.1	VS, FV
D	Mus. 1µg/µl	1	Left	1	10	5.8	VS, FV
D	Mus. 1µg/µl	1	Right	2	10	6.2	VS, FV
D	Mus. 1µg/µl	1	Right	2	10	5.7	VS, FV
D	Mus. 1µg/µl	1	Right	1	10	6.4	VS, FV
D	Saline	1	Right	2	10	6.3	VS, FV
D	Saline	1	Right	0	10	6.5	VS
D	Saline	1	Right	0	10	6.3	VS, FV
D	Saline	1	Right	2	10	6.5	VS, FV
D	Saline	1	Left	1	8	6.7	VS, FV
D	Saline	1	Left	0	9	6.9	VS, FV
S	Mus. 5µg/µl	1	Left	1	9.5	5	VS, FV
S	Mus. 5µg/µl	1	Right	3	11.5	6.2	FV
S	Mus. 5µg/µl	1	Right	1	9.5	6.4	VS, FV
S	Mus. 5µg/µl	1	Right	1	9.5	6.7	VS, FV
S	Saline	1	Left	1	9.5	6.5	VS, FV
S	Saline	1	Right	1	9.5	6.2	VS, FV
S	Saline	1	Right	2	10.5	6.5	VS, FV
S	Saline	1	Left	2	7.5	6.4	VS, FV

Table S2 (related to Figures 1-6)
Statistic values. (the file was provided separately as an Excel table)

Table S3 (related to Figure 4)
Injection sites of the viral vector for optogenetic experiments. AC: anterior commissure. The positions listed below are chamber coordinates, which were tilted 15 degrees anteriorly relative to the stereotaxic reference frame (millimeter).

Monkey	Volume (μl)	Injection side	Posterior from AC (mm)	Lateral from midline (mm)	Depth from AC (mm)
D	2	Right	1	10	7.1
D	2	Right	2	9	7.1
S	3	Left	2	9.5	6.5
S	2	Left	1	10.5	6.5
S	2	Left	3	10.5	7

TRANSPARENT METHODS

Subjects and surgery

We used two rhesus monkeys (Macaca mulatta) (monkey S: 8.5 kg, 7y old, male, monkey D: 5.0 kg, 13y old, female). All animal care and experimental procedures were approved by the National Eye Institute Animal Care and Use Committee and complied with the Public Health Service Policy on the Humane Care and Use of Laboratory Animals. Both animals underwent surgery under general anesthesia during which a head holder and a recording chamber were implanted on the head. Based on a stereotaxic atlas (Saleem and Logothetis, 2007), we implanted a rectangular chamber targeting the amygdala. The chamber was tilted anteriorly by 15 degrees in both monkeys. After confirming the position of recording chamber using MRI (4.7 T, Bruker), a craniotomy was performed during a second surgery.

Neuronal recording

Single-unit recording was performed using glass-coated electrodes (Alpha-Omega). The electrode was inserted into the brain through a stainless-steel guide tube and advanced by an oil-driven micromanipulator (MO-97A, Narishige). The recording sites were determined by using a grid system that allowed recordings at 1-mm intervals in x- and y-directions, orthogonal to the guide tube. The input from the electrode was amplified (A-M Systems) with a band-pass filter (0.2–10 kHz; BAK). Neuronal spikes were isolated online using custom software implementing a voltage and time window discriminator (Blip). We identified amygdala and the surrounding areas (striatum, GPe, and SNr) based on MRI images and characteristic firing patterns in neurophysiological recordings. The MR images were obtained in sections parallel to the recording chamber, which was visualized with gadolinium that filled grid holes and the space outside the grid and inside the chamber. As the electrode was advanced, the characteristic activity of GPe neurons (high-frequency tonic firing around 30-100 Hz, and occasional pauses) faded (Hong and Hikosaka, 2008). Then, after the electrode passed through a quiet white matter region, spikes of amygdala neurons (heterogeneous firing patterns, relatively consistent firing with no pause) grew larger. The striatum includes the following characteristic activities. Medium spiny neurons were identified by their low baseline activity (1-10 Hz) and broad action potentials (Kunimatsu et al., 2019). Tonically active neurons exhibited a characteristic tonic firing pattern and wider action potentials. Fast-spiking interneurons exhibited high baseline activity (around 30-80 Hz) and a sharp spike shape. SNr neurons exhibited consistent and high baseline activity (Yasuda et al., 2012).

Muscimol injections

Head position was stabilized throughout the experimental session by means of a chronically implanted head post. After the electrophysiological recording of amygdala neurons in both monkeys, we performed inactivation experiments to test for a causal relationship between amygdala neuronal activity and eye movements. We also inactivated surrounding areas of the amygdala (GPe and Striatum). To accurately inactivate the brain structure, we used an electrode assembly (injectorode) consisting of an epoxy-coated tungsten microelectrode (FHC) for unit recording and a polyimide tube (MicroLumen) for drug delivery. After the precise identification of the recording areas by unit recording, we injected the $GABA_A$ receptor agonist muscimol (Sigma, MO, USA) into the amygdala (8.8 nmol [1µg] or 44 nmol [5 µg] in a 1 µl volume) or other areas (44 nmol [5 µg] in a 1 µl volume) in one hemisphere at the speed of 0.2 ml/min by a 10 µl Hamilton syringe and manual infusion pump (Stoelting, IL, USA). Because the effect of muscimol on the amygdala lasted for several hours, inactivation sessions were limited to twice per week. The order of these injections was alternated. The minimum actual time between inactivation sessions was one day. Soon after the injection was completed (within 5 min), the animal was invited to start several tasks and repeat performance after periodic rest breaks every 20-60 min for 3-5 hr. In this experiment, we used a visually-guided saccade task and a free-viewing task to analyze the effects of inactivation on eye-movements. To show injection sits and recording sites on an image (Figure 1 and Figure S7), we first identified the anterior commissure and the amygdala on coronal sections of MR images in each monkey. Then, image co-registration was performed for these images based on the landmarks and superimposed by overlay function in Photoshop (Adobe Inc).

Viral injections and optogenetics

After the muscimol injection experiments were completed, we injected an adeno-associated virus type 2 vector (AAV2-CMV-ChR2-EYFP: 9.0 x 10_{12} genome copy/ml) into the amygdala area of one hemisphere in both monkeys (monkey S: left amygdala, monkey D: right amygdala). The vector was successfully used

in the macaque brain in a previous study (Inoue et al., 2015). Two penetrations in monkey D and three penetrations in monkey S were made into one side of amygdala at least 1.41 mm apart from each other. For each penetration, 2 µl (for monkey D) and 2 or 3 µl (for monkey S) of the vector were introduced at a rate of 0.4 µl/min for the first 0.2 µl, followed by 0.08 µl/min for the remainder of the injection controlled by a 10 µl Hamilton syringe and motorized infusion pump (Harvard Apparatus, Holliston, MA, USA).
For optical stimulation and electrophysiological recording, we used optrodes consisting of an epoxy-coated tungsten microelectrode (FHC) for unit recording and an optic fiber (200 µm diameter, Doric Lenses) for optical stimulation using laser light. The light sources were 473nm DPSS blue light lasers with a maximum power of up to 100mW (Opto Engine LLC). We left the laser on continuously during the experiment and placed a mechanical switcher (Luminos Industries Ltd) in the light path to turn the laser on and off. We measured the light intensity at the tip of the optrode before penetration of the brain using an optical power meter (1916-C, Newport Corporation) coupled with a 818-SL/DB photo detector. The light intensities were 30-50 mW/mm_2 for amygdala neurons and 300-500 mW/ mm_2 for other projection sites (GPe, Striatum, and SNr). The maximum light intensity in each site was used for the controls as for the amygdala and SNr optical stimulations (50 mW/mm_2 and 500 mW/ mm_2, respectively). Stimulation and non-stimulation periods were pseudo-randomly interleaved 100 times while the monkey was freely viewing during multiple visual stimulation regimes presented at random, including pictures, a blank screen, and the videos shown in the free-viewing task.

Histology
After completing all experiments, one subject (monkey D) was deeply anesthetized with an overdose of sodium pentobarbital (390 mg/ml) and perfused transcardially with saline followed by 4% paraformaldehyde. The head was fixed to the stereotaxic frame, and the brain was cut into blocks in the coronal plane including midbrain region. The block was post-fixed overnight at 4 C°, and then cryoprotected for one week in increasing gradients of glycerol solution (10 to 20% glyceorol in PBS) before being frozen. The frozen block was cut into 50 µm sections using a microtome. Slices taken at 250 µm-intervals were used for identifying EYFP signals and the adjacent slices were used for Nissl staining. We captured the fluorescent images of the labeled neurons and Nissl staining images using two different microscopes (Leica SP8 and Keyence BZ-X700). EYFP signals were excited by 514 nm wavelength laser and detected by HyD sensor (range from 519 nm to 640 nm wavelength). Autofluorescence signals were excited by same wavelength laser and detected by HyD sensor (range from 646 nm to 794 nm wavelength). We adjusted the contrast and brightness of each color channel using Photoshop (Adobe) to enhance the ability to identify fluorescently labeled neurons.

Immunofluorescence histochemistry
For enhancing the EYFP signals, we used rabbit anti-GFP antibody (G10362; Thermo Fisher) and goat anti-rabbit IgG antibody conjugated with Alexa fluor 488 (A-11034; Thermo Fisher). The sections were preincubated for 30 min in 0.3 % hydrogen peroxide in 0.1 M PBS (pH 7.4) to block endogenous peroxidase, followed by three rinses through 0.1 M PBS, and then 1 hour in blocking solution containing 5% normal goat serum in 0.1 M PBS. The sections were incubated for 18 hours at room temperature in blocking solution containing 2.5% normal goat serum and 0.1% TX-100 with rabbit anti-GFP antibody (1:2000). After three rinses with PBS, the sections were incubated for 2 hours at room temperature with goat anti-rabbit IgG antibody conjugated with Alexa fluor 488 (1:200). To visualize colocalization of ChR2-EYFP and neurons accurately, we have done double-staining by using chicken anti-NeuN antibody (1:500; ABN91, Millipore) and goat anti-chicken IgY (IgG) conjugated with Alexa fluor 594 (1: 200, A-11042; Thermo Fisher) in addition to the above method. We captured the fluorescent images of the labeled neurons and axons using the microscopes (SP8, Leica), range from 493 nm to 601 nm wavelength for the Alexa fluor 488 signals and range from 607 nm to 746 nm wavelength for autofluorescence signals or range from 596 nm to 760 nm wavelength for Alexa fluor 594. We adjusted the contrast and brightness of each color channel using Photoshop (Adobe) to enhance the ability to differentiate fluorescently labeled neurons.

Experimental control
All behavioral tasks were controlled by a custom neural-recording and behavior-controlling system (Blip; available at http://www.robilis.com/blip/). The monkey sat in a primate chair facing a fronto-parallel screen in a sound-attenuated and electrically shielded room. Visual stimuli were rear-projected onto a screen by

a digital light processing projector (PJD8353s, ViewSonic). Eye position was sampled at 1 kHz using a video-based eye tracker (EyeLink 1000 Plus, SR Research).

Foraging task

We previously devised a foraging task in which the monkeys viewed many scenes presented in randomized order across different trials and made saccades to good objects to receive rewards (Maeda et al., 2018). The detailed descriptions of methods should be referred to the paper. After a blank screen (inter trial interval 4 – 8 sec.), a scene appeared suddenly, and the subject was allowed to view the scene freely for 1,080 ms (FV period). Then, a fixation point (FP) appeared at the center. If the subject held its gaze on the FP for 780 ms (FX period), an object appeared at the same time as the FP disappeared. The object appearance was random and unpredictable in two ways: (1) sequence: two or three objects contained in the scene appeared randomly in sequence and (2) position: the objects appeared randomly at one of eight positions (eccentricity: 15 deg; angle: in steps of 45 deg from straight up). Each scene contained at least two objects with different features. Objects #1 and #2 were responsive to the subject's choice (i.e., sustained gaze, when the monkey made a saccade to it within 1,000 ms and kept fixating for >400 ms). Saccades to object #1 gave the subject a reward (called "good" object), whereas saccades to object #2 gave no reward (called "bad" object). Thus, the subject's goal was to make saccades to object #1 but not object #2. Such objects were present in all scenes, although they were visually different. Some scenes also contained the third object (object #3, "robber"). After the robber object appeared, it remained in place (irrespective of the subject's eye movements) until either the good or the bad object appeared. If the bad object appeared, the robber object did nothing, and the subject simply needed to make no action before FP reappeared. If the good object appeared, the robber was programmed to jump across the screen and intercept the object with timing designed to race against the monkey's saccade to the good object. On trials in which the robber's jump preceded the monkey's response, the robber "stole" the reward that would otherwise follow a correct saccade to the good object. Stolen trials occurred if the subject's saccade was delayed (reaction time: >105 – 135 ms for monkey D, >95 – 125 ms for monkey SO; the threshold was random across trials between these numbers). Otherwise, the subject obtained the reward. If the subject failed (i.e., the robber beat the saccade), the same trial was repeated in the same sequence until a successful trial occurred (i.e., the saccade beat the robber), but these repeated trials were not included in behavioral and neuronal analysis. To encourage the subject, the criterion reaction time was incremented by 10 ms after each failure. Based on the effects of these objects, the scenes were classified into three contexts. In the Safe and Rich (S/R) context, the good object was associated with a big reward (0.3 mL) and the robber object never appeared. In the Safe and Poor (S/P) context, the good object was associated with a small reward (0.1 mL) and the robber object never appeared. In the Dangerous and Rich (D/R) context, the good object was associated with a big reward (0.3 mL) and the robber object might appear but only did so on around 30 % of the trials randomly.

Visually-guided saccade task

Trials began with the appearance of a central fixation point. After the monkey fixated for 770 ms the fixation point disappeared, and a saccade target (2 x 2 degree) was presented at one of six positions randomly. The monkey was required to make a saccade and maintain fixation for 400 ms within the target window (10 x 10 degree) to obtain a water reward (0.1 mL). In Figure S3, two different reward amounts were used (0.08 and 0.15 mL for low- and high-valued object, respectively).

Free-viewing task

The monkey freely watched a movie without any rewards. The movie consisted of several video clips and lasted 5 minutes (30 frames/sec), mostly showing macaque monkeys engaged in natural behavior. We used the same movie across experiments. The video clips were assembled from commercially available documentaries and wildlife footage and previously used in another study (McMahon et al., 2015). The movie was presented within a rectangular frame of 46° wide and 34° high by custom-written MATLAB functions.

Data analysis for neuronal responses

To find visually responsive amygdala neurons, we let the monkey continue to perform the foraging task and checked responses to scene images and object images. We examined any neuron systematically if it responded to at least one scene image using the foraging task. Some SNr neurons were examined in the

foraging task while the neurons were modulated by optogenetic stimulation. We compared the responses of amygdala or SNr neurons to different contexts as well as individual scenes. To assess effects on neuronal activity that were purely attributable to scene images in the foraging task, we set a test window immediately before the saccade to the first object during FX period (200 ms before the object onset). We calculated the mean firing rate evoked by each scene for each neuron, which was converted to normalized rates: (FRi − FRb) / SD, (FRi: mean firing rate during the test window, FRb: baseline firing rate, SD: standard deviation of mean firing rates for all scenes). We then averaged normalized rates of all scene-responsive neurons for each context of scenes and for each scene. To examine the significance of context discrimination we used a one-way ANOVA (three groups [D/R, S/R, S/P], post hoc: Tukey–Kramer).
To investigate neuronal responses to the optical stimulation, we compared neuronal activities in a 200 ms test window after the stimulation onset with a baseline window (0–500 ms before the stimulation onset) for each neuron. Neuronal responses were considered significant whenever the corresponding statistics was associated with a P value that was less than 0.05 (t-test, inhibition or excitation; Figure 4 and 5).

Data analysis for saccade
In the visually-guided saccade task and foraging task, saccade latency was measured as the time between the offset of the fixation point (simultaneous with the onset of the object) and the onset of the saccade to the object. To determine effects on saccade latency purely attributable to scene images or contexts in the foraging task, the latency was measured only for saccades to the first good object in each trial. First, saccades were detected when the peak velocity of the eye trace exceeded 300 degrees/s. Saccade onset time was defined as the time point preceding the detected saccade at which the velocity exceeded 30 degrees/s. In the free-viewing task, we analyzed saccades with amplitudes ranging from 5 to 40 degrees. To calculate the gaze shift index, the gaze probability on the ipsilateral side in the injection condition was divided by the probability in the condition without injection. In the optogenetic stimulation experiments, differences in the cumulative number of saccades between stimulation and control conditions were plotted, including all sessions in each monkey. Saccadic eye movements to right and left directions were applied to positive and negative numbers, respectively. Positive values indicate more saccadic eye movements to right side compared with control data, and vice versa.

Data analysis for heart rate
Heart rate was measured by using a pulse sensor (World Famous Electronics llc) at the ear. The signals that were more than three times the median absolute deviations away from the median were removed as outliers in each trial. Then, a vector with the local peaks of the signals was returned to calculate inter-pulse intervals and converted to beats per minute. Outlier inter-pulse intervals were detected and removed when the duration was more than 450 ms. To determine effects on heart rate purely attributable to scene images or contexts before saccade initiation in the foraging task, we only used a most recent inter-pulse interval before first object onset in the FX period in each trial.

Supplemental References
Hong, S., and Hikosaka, O. (2008). The Globus Pallidus Sends Reward-Related Signals to the Lateral Habenula. Neuron *60*, 720-729.

Inoue, K.-i., Takada, M., and Matsumoto, M. (2015). Neuronal and behavioural modulations by pathway-selective optogenetic stimulation of the primate oculomotor system. In Nat Commun, pp. 8378.

Kunimatsu, J., Maeda, K., and Hikosaka, O. (2019). The Caudal Part of Putamen Represents the Historical Object Value Information. The Journal of neuroscience : the official journal of the Society for Neuroscience *39*, 1709-1719.

Maeda, K., Kunimatsu, J., and Hikosaka, O. (2018). Amygdala activity for the modulation of goal-directed behavior in emotional contexts. In PLoS Biol, pp. e2005339.

McMahon, D.B.T., Russ, B.E., Elnaiem, H.D., Kurnikova, A.I., and Leopold, D.A. (2015). Single-unit activity during natural vision: diversity, consistency, and spatial sensitivity among AF face patch neurons. In J Neurosci, pp. 5537-5548.

Yasuda, M., Yamamoto, S., and Hikosaka, O. (2012). Robust representation of stable object values in the oculomotor Basal Ganglia. The Journal of neuroscience : the official journal of the Society for Neuroscience *32*, 16917-16932.